SAR COMPLIANCE TESTING OF WISTRON NEWEB CORPORATION MODEL EM-500

AG 802.11 a/b/g MINI PCI CARD BUILT INTO MODEL BQ12 NOTEBOOK COMPUTER

FCC ID: NKRBQ12AB
Host Computer: Model BQ12

February 28, 2003

Prepared for:

Wistron NeWeb Corporation
No. 10-1, Li-hsin Road 1
Science-Based Industrial Park
Hsinchu, 300
Taiwan, R.O.C.
Attention: Eric Y.C. Liu
Senior Manager, Engineering

Prepared by:

Om P. Gandhi
Professor of Electrical and Computer Engineering
University of Utah
50 S Central Campus Dr., Rm. 3280
Salt Lake City, UT 84112-9206

TABLE OF CONTENTS

SAR COMPLIANCE TESTING OF WISTRON NEWEB CORPORATION MODEL EM-500 AG 802.11 a/b/g MINI PCI CARD BUILT INTO MODEL BQ12 NOTEBOOK COMPUTER

FCC ID: NKRBQ12AB
Host Computer: Model EM-500 AG

I. Introduction

The U.S. Federal Communications Commission (FCC) has adopted limits of human exposure to RF emissions from mobile and portable devices that are regulated by the FCC [1]. The FCC has also issued Supplement C (Edition 97-01) to OET Bulletin 65 [2] and a more recent version of the same [3] defining both the measurement and the computational procedures that should be followed for evaluating compliance of mobile and portable devices with FCC limits for human exposure to radiofrequency emissions.

We have used the measurement procedure for SAR compliance testing of the Wistron NeWeb Model EM-500 AG 802.11 a/b/g Mini PCI Card built into Model BQ12 Notebook Computer (FCC ID# NKRBQ12AB). The photographs of the Model BQ12 Notebook Computer with built-in Model EM-500 AG 802.11a Wireless Antennas are given in Figs. 1a, b, c, and Fig. 2, respectively. As seen in Fig. 2, two 802.11a antennas marked "Main" and "Aux" (auxiliary) antennas are built close to the right and left edges of the keyboard, respectively. Even though two 802.11a antennas are built into the base of the PC for diversity, only one of the two antennas are active at any given time. Each of the Wistron Model EM-500 AG 802.11a wireless antennas operates over the frequency band 5.15 to 5.35 GHz in base or turbo modes with conducted power levels given in Table 1.

For SAR measurements, two configurations of the wireless PC relative to the experimental phantom have been used. These are as follows:

a. **Configuration 1** is for the wireless PC placed on a user's lap. For this configuration, a planar phantom model with inside dimensions 12" x 16.5" (30.5 x 41.9 cm) and a base thickness of 2.0 ± 0.2 mm (recommended in [3]) was used for SAR measurements and the bottom side of the laptop computer shown in Fig. 1b was pressed against it. The

SARs were measured both for the "Main" and "Aux" (auxiliary) antennas individually (see Figs. 3a, b).

b. **Configuration 2** -- Edge-on position. This configuration corresponds to a bystander close to the right or left edges of the PC base at a distance of 1.5 cm. For this configuration, the right or the left edge of the PC base is placed at 90° relative to the flat phantom at a distance of 1.5 cm as shown in Figs. 4a, b, respectively.

II. The SAR Measurement System

The University of Utah SAR Measurement System has been described in peer-reviewed literature [Ref. 8 -- attached here as Appendix A]. A photograph of the SAR Measurement System is given in Fig. 5. This SAR Measurement System uses a computer-controlled 3-D stepper motor system (Arrick Robotics MD-2A). A triaxial Narda Model 8021 E-field probe is used to determine the internal electric fields. The positioning repeatability of the stepper motor system moving the E-field probe is within ±0.1 mm. Outputs from the three channels of the E-field probe are dc voltages, the sum of which is proportional to the square of the internal electric fields $\left(|E_i|^2\right)$ from which the SAR can be obtained from the equation SAR = $\sigma\left(|E_i|^2\right)\Big/\rho$, where σ and ρ are the conductivity and mass density of the tissue-simulant materials, respectively [5]. The dc voltages for the three channels of the E-field probe are read by three HP 34401A multimeters and sent to the computer via an HPIB interface. The setup is carefully grounded and shielded to reduce the noise due to the electromagnetic interference (EMI). A cutout in a wooden table of dimensions 38.1 × 21.6 cm allows placement of a plastic holder (shown in Fig. 6) on which the laptop computer with the 802.11 a/b wireless antennas (see Figs. 1 and 2) is supported. A plastic holder (see Fig. 6) can be moved up or down so that the base of the PC (for Configuration 1) is pressed against the base of the flat phantom for determination of SAR for Above-Lap position. Similarly, for "Edge-On" SAR determination, Configuration 2, the laptop computer is mounted sideways (at 90°) on the plastic holder and moved up so that the

right or the left edge of the keyboard base with the 802.11 a/b main or auxiliary wireless antennas was parallel to the bottom of the flat phantom with a spacing of 1.5 cm (see Figs. 4a, b).

The Flat Phantom

As recommended in Supplement C Edition 01-01 to OET Bulletin 65 [3], a planar phantom model with inside dimensions 12" × 16.5" (30.5 × 41.9 cm) and base thickness 2.0 ± 0.2 mm was used for SAR measurements (see Figs. 3-5).

III. Calibration of the E-Field Probe

The IEEE Draft Standard P1528 [4] suggests a recommended procedure for probe calibration (see Section 4.4.1 of [4]) for frequencies above 800 MHz where waveguide size is manageable. Calibration using a rectangular waveguide is recommended. As in some previously reported SAR measurements at 6 GHz [5], we have calibrated the Narda Model 8021 Miniature Broadband Electric Field Probe of tip diameter 4 mm (internal dipole dimensions on the order of 2.5 mm) using a rectangular waveguide WR 159 (of internal dimensions 1.59 x 0.795 inches) that was filled with the tissue-simulant fluid of composition given in Section V (see Figs. 7a, b). The triaxial (3 dipole) E-field probe shown in Fig. 8 was originally developed by Howard Bassen and colleagues of FDA and has been manufactured under license by Narda Microwave Corporation, Hauppage, New York. The probe is described in detail in references 6 and 7. It uses three orthogonal pick up dipoles each of length about 2.5 mm offset from the tip by 3 mm, each with its own leadless zero voltage Schottky barrier diode operating in the square law region. The sum of the three diode outputs read by three microvoltmeters [8] gives an output proportional to E^2. By rotating the probe around its axis, the isotropy of the probe was measured to be less than ± 0.23 dB and the deviation of the probe from the square law behavior was less than ± 3%.

As suggested in the Draft Standard P1528, the waveguide (WR 159) filled with the tissue-simulant fluid was maintained vertically. From microwave field theory [see e.g. ref. 9], the transverse field distribution in the liquid corresponds to the fundamental mode (TE_{10}) with

an exponential decay in the vertical direction (z-axis). The liquid level was 15 cm deep which is deep enough to guarantee that reflections from the top liquid surface do not affect the calibration. By comparing the square of the decaying electric fields expected in the tissue from the analytical expressions for the TE_{10} mode of the rectangular waveguide, we obtained a calibration factor of 2.98 (mW/kg)/μV with a variability of less than ±2% for measurement frequencies of 5.2 and 5.3 GHz, respectively. This is no doubt due to a fairly limited frequency band of only 0.1 GHz out of a recommended bandwidth of 2.2 GHz for the TE_{10} mode for the WR159 waveguide (recommended band of 4.9-7.1 GHz -- see e.g. ref. 9) and the fact that the bandwidth of 600 MHz for the entire set of measurements is on the order of ± 5.5% of the midband frequencies..

The date for the calibration of the E-field probe closest to the SAR tests given here was February 26, 2003.

IV. SAR System Verification

Since we do not have a dipole for the 5 GHz band, a half wave dipole at 1900 MHz was used instead for SAR system verification. This dipole of length 76.0 mm and diameter 1.5 mm and h = 39.5 mm is shown in Fig. 9. As recommended in OET65 Supplement C [3], we used a spacing of 10 mm from the dipole to the tissue-simulant fluid composed of 40.4% water, 58.0% sugar, 0.5% salt (NaCl), 1% HEC, and 0.1% bactericide. The microwave circuit arrangement used for system verification is sketched in Fig. 10. The dielectric properties for this body-simulant fluid were measured using the Hewlett Packard (HP) Model 85070 B Dielectric Probe (rated frequency band 200 MHz to 20 GHz in conjunction with HP Model 8720C Network Analyzer (50 MHz-20 GHz) using a procedure detailed in Section V. The measured dielectric parameters of the body-simulant fluid at 1900 MHz are $\varepsilon_r = 53.1 \pm 1.3$ and $\sigma = 1.44 \pm 0.09$ S/m. The measured properties are close to the values of $\varepsilon_r = 54.0$ and $\sigma = 1.45$ S/m given in OET Supplement C [3].

The measured SAR distribution for the peak 1-g SAR region using this system verification dipole for the day of SAR measurements, February 26, 2003, is given in Appendix

B. Also given in Appendix B is the dipole SAR plot for this date of device testing. The peak 1-g SAR is 36.463 W/kg. The measured 1-g SAR is in excellent agreement with the FDTD-calculated 1-g SAR of 35.8 W/kg for this dipole. Also as expected, the measured SAR plot is quite symmetric.

V. Tissue Simulant Fluid for the Frequency Band 5.2 to 5.8 GHz

In OET 65 Supplement C [3], the dielectric parameters suggested for body phantom are given only for 3000 and 5800 MHz. These are listed in Table 2 here. Using linear interpolation, we can obtain the dielectric parameters to use for the frequency band between 5.2 to 5.4 GHz. The desired dielectric properties thus obtained are also given in Table 2. From Table 2, it can be noticed that the desired dielectric constant ε_r varies from 48.7 to 49.0 which is a variation of less than ± 1% from the average value of 48.9 for this band. Also the conductivity σ varies linearly with frequency from 5.3 to 6.00 S/m. For the SAR measurements given in this report, we have used a tissue-simulant fluid developed at the University of Utah which consists of 68.0% water, 31.0% sugar and 1% HEC. For this composition, we have measured the dielectric properties using a Hewlett Packard (HP) Model 85070B Dielectric Probe in conjunction with HP Model 8720C Network Analyzer (50 MHz-20 GHz). The measured dielectric properties at a mid band frequency of 5.30 GHz are as follows: $\varepsilon_r = 48.5 \pm 1.7$ and $\sigma = 5.40 \pm 0.08$ S/m. From Table 2, we obtain the desired dielectric properties to simulate the body tissue at the midband frequency of 5.30 GHz to be $\varepsilon_r = 48.9$ and $\sigma = 5.42$ S/m. Thus, the measured properties for the body-simulant fluid are close to the desired values. Also as expected, the conductivity of this fluid varies linearly with frequency rising to 5.61 ± 0.09 S/m at 5.4 GHz, while the dielectric constant ε_r is nearly the same as the measured value at 5.3 GHz.

The procedure is as follows: The HP Model 95070B Dielectric Probe (see Fig. 11) is an open-circuited transmission-line (coaxial line) probe similar to that described in Section B.1.2 of the Draft IEEE Standard 1528 [4]. The theory of the open-circuited coaxial line method has been described in scientific literature [10-12]. We have previously used this method in

determining the dielectric properties of tissue-simulant materials at 6 GHz [5]. In this method, the complex reflection coefficient Γ^* measured for the open end of the coaxial line can be used to calculate the complex permittivity ε* from the following equation [5]

$$\varepsilon^* = \frac{1-\Gamma^*}{j\omega Z_o C_o \left(1+\Gamma^*\right)} - \frac{C_f}{C_o} \tag{1}$$

where Z_o is the characteristic impedance (50 Ω) for the coaxial line, C_o is the capacitance when the line is in air and C_f is the capacitance that accounts for the fringing fields in the dielectric of the coaxial line.

For the HP85070B Dielectric Probe with diameters of the outer and inner conductors 2b = 3.00 mm and 2a = 0.912 mm, respectively, the following capacitances were obtained using deionized water and methanol as the calibration fluids. The following capacitances were obtained:

$$C_o = 0.022 \text{ pF}$$

$$C_f = 0.005 \text{ pF}$$

Using the network analyzer HP8720C, we measured the reflection coefficient Γ^* for the open end of the coaxial line that was submerged in the tissue-simulant fluid. Using Eq. 1, the complex permittivity of the fluid was measured at various frequencies 5.2-5.4 GHz. From the imaginary part of the complex permittivity Im(ε^*), we can obtain the conductivity σ from the relationship

$$\sigma = \frac{\text{Im}(\varepsilon^*)}{\omega \varepsilon_o} \tag{2}$$

VI. The Measured SAR Distributions

The RF power output measured for the Wistron NeWeb 802.11a Wireless Antenna is given in Table 1. For SAR measurements, we selected frequencies of 5.26 GHz for the base mode and 5.29 GHz for the turbo mode. These frequencies and modes were selected both for

their highest power outputs as well as to cover the different frequency modes planned for this wireless device. As recommended in Supplement C, Edition 01-01 [3], the stability of the conducted power was determined by repeated SAR measurements at the same location for each of the selected channels. The variability of the SAR thus determined for three repeated measurements over a 60-minute time period was within ± 0.1 dB (± 2.5%).

The highest SAR region for each of the measurement frequencies was identified in the first instance by using a coarser sampling with a step size of 8.0 mm over three overlapping areas for a total scan area of 8.0 × 9.6 cm. The data thus obtained is resolved into a 4 x 4 times larger grid i.e. a grid involving 40 x 28 points by linear interpolation using a 2 mm step size. After thus identifying the region of the highest SAR, the SAR distribution was then measured with a resolution of 2 mm in order to obtain the peak 1 cm^3 or 1-g SAR. The SAR measurements are performed at 4, 6, 8, 10, 12 mm height from the bottom surface of the body-simulant fluid. The SARs thus measured were extrapolated using a second-order least-square fit to the measured data to obtain values at 1, 3, 5, 7 and 9 mm height and used to obtain 1-g SARs. The uncertainty analysis of the University of Utah SAR measurement system is given in Appendix C. The combined standard uncertainty is ± 8.3%.

As previously mentioned, two Wistron NeWeb 802.11 a/b antennas are built close to the two edges of the keyboard base for this PC (see Fig. 2). Even though two 802.11a antennas marked "Main" and "Aux" (auxiliary) are built into the base of the PC for diversity, only one of the two antennas are active at any given time. For the present measurements, we have determined the SAR distributions for the Main and the Auxiliary antennas for the Lap-top and Edge-on positions, respectively. The coarse scans for the four measurements for the Lap-top Configuration 1 (defined in Section I) are shown in Fig. 12a-d, respectively. In these figures, the two axes are marked in units of the step size of 8 mm. The highest SAR region shown in maroon color is immediately above the region of the radiating antenna as illustrated in Fig. 2. Given in Tables 3-6 are the SAR distributions for the peak SAR region of volume 10 ×10 × 10 mm for which the coarse scans are given in Figs. 12a-d, respectively. The SARs are

given for xy planes at heights z of 1, 3, 5, 7, and 9 mm from the bottom of the flat phantom. The individual SAR values for this grid of 5 × 5 × 5 or 125 points are averaged to obtain peak 1-g SAR values (for a volume of 1 cm^3). The temperature variation of the tissue-simulant fluid measured with a Bailey Instruments Model BAT 8 Temperature Probe over the 80-minute period needed for measurements at the four frequencies was $23.2 \pm 0.2^{\circ}C$.

The coarse scans measurements for the four measurements for the Edge-on Configuration 2 are shown in Fig. 13a-d, respectively. The corresponding SAR distributions for the peak 1-g SAR are given in Tables 7-10, respectively. As mentioned in Section I, this Configuration 2 corresponds to the placement of the right or left edge of the PC at 90° at a distance of 1.5 cm from the bottom of the flat phantom (see Figs. 4a and 4b). This configuration corresponds to a situation when a bystander is standing close to the right or the left edges of the PC base at a distance of 1.5 cm. The z-axis scan plots taken at the highest SAR locations for each set of tests are given in Fig. 14 and 15, respectively.

The peak 1-g SARs for the various configurations of the Wistron NeWeb Model BQ12 Notebook PC (FCC ID# NKRBQ12AB) are summarized in Table 11. All of the measured 1-g SARs are less than the FCC 96-326 guideline of 1.6 W/kg.

VII. Comparison of the Data with FCC 96-326 Guidelines

According to the FCC 96-326 Guideline [1], the peak SAR for any 1-g of tissue should not exceed 1.6 W/kg. For the Wistron NeWeb Model BQ12 Notebook PC (FCC ID# NKRBQ12AB), the measured peak 1-g SARs vary from 0.125 to 0.909 W/kg which are smaller than 1.6 W/kg.

REFERENCES

1. Federal Communications Commission, "Guidelines for Evaluating the Environmental Effects of Radiofrequency Radiation," FCC 96-326, August 1, 1996.

2. K. Chan, R. F. Cleveland, Jr., and D. L. Means, "Evaluating Compliance With FCC Guidelines for Human Exposure to Radiofrequency Electromagnetic Fields," Supplement C (Edition 97-01) to OET Bulletin 65, December, 1997. Available from Office of Engineering and Technology, Federal Communications Commission, Washington D.C., 20554.

3. Federal Communications Commission "Supplement C Edition 01-01 to OET Bulletin 65 Edition 97-01" June 2001.

4. IEEE Draft Standard P1528, "Recommended Practice for Determining the Peak Spatial-Average Specific Absorption Rate (SAR) in the Human Body Due to Wireless Communication Devices: Experimental Techniques," Draft CBD1.0, April 4, 2002 (IEEE Standards Coordinating Committee 34).

5. O. P. Gandhi and J-Y. Chen, "Electromagnetic Absorption in the Human Head from Experimental 6-GHz Handheld Transceivers," *IEEE Transactions on Electromagnetic Compatibility*, Vol. 39(4), pp. 547-558, 1995.

6. H. Bassen. M. Swicord, and J. Abita, "A Miniature Broadband Electric Field Probe," Ann. New York Academy of Sciences, Vol. 247, pp. 481-493, 1974.

7. H. Bassen and T. Babij, "Experimental Techniques and Instrumentation," Chapter 7 in *Biological Effects and Medical Applications of Electromagnetic Energy*, O. P. Gandhi, Editor, Prentice Hall Inc., Englewood Cliffs, NJ, 1990.

8. Q. Yu, O. P. Gandhi, M. Aronsson, and D. Wu, "An Automated SAR Measurement System for Compliance Testing of Personal Wireless Devices," *IEEE Transactions on Electromagnetic Compatibility,* Vol. 41(3), pp. 234-245, August 1999 (attached as Appendix A).

9. O. P. Gandhi, *Microwave Engineering and Applications,* Pergamon Press, New York, 1981.

10. T. W. Athey, M. A. Stuchly, and S. S. Stuchly, "Measurement of Radiofrequency Permittivity of Biological Tissues with an Open-Circuited Coaxial Line - Part I," *IEEE Transactions on Microwave Theory and Techniques*, Vol. MTT-30, pp. 82-86, 1982.

11. M. A. Stuchly, T. W. Athey, G. M. Samaras, and G. E. Taylor, "Measurement of Radiofrequency Permittivity of Biological Tissues with an Open-Circuited Coaxial Line - Part II - Experimental Results," *IEEE Transactions on Microwave Theory and Techniques*, Vol. MTT-30, pp. 87-92, 1982.

12. C. L. Pournaropoulos and D. K. Misra, "The Coaxial Aperture Electromagnetic Sensor and Its Application for Material Characterization," *Measurement Science and Technology*, Vol. 8, pp. 1191-1202, 1997.

Table 1. Average conducted RF power outputs measured at various frequencies for the Wistron NeWeb 802.11a Wireless Antennas for base and turbo modes.

Frequency GHz	Average Power dBm
Normal Mode	
5.18 5.26 5.32	16.5 18.8 18.3
Turbo Mode	
5.21 5.25 5.29	16.2 16.3 17.4

Table 2. Dielectric parameters for body phantom for the frequency band 5.2 to 5.8 GHz [3].

Frequency GHz	ε_r	σ S/m	Reference
3.0	52.0	2.73	Ref. 3
5.8	48.2	6.00	Ref. 3
5.2	49.0	5.30	Interpolated
5.3	48.9	5.42	Interpolated
5.4	48.7	5.53	Interpolated

Table 3. **Above-Lap position (Configuration 1).** The SARs measured for the Wistron NeWeb Model BQ12 802.11a **Main** Wireless Antenna for the base mode at 5.26 GHz.

1-g SAR = 0.223 W/kg

a. At depth of 1 mm

0.338	0.305	0.326	0.318	0.320
0.319	0.320	0.326	0.347	0.319
0.325	0.321	0.313	0.339	0.325
0.291	0.325	0.329	0.321	0.328
0.291	0.324	0.321	0.310	0.298

b. At depth of 3 mm

0.272	0.257	0.262	0.263	0.259
0.263	0.263	0.264	0.268	0.263
0.261	0.260	0.254	0.268	0.255
0.241	0.261	0.268	0.260	0.257
0.240	0.254	0.253	0.249	0.242

c. At depth of 5 mm

0.220	0.217	0.211	0.219	0.212
0.218	0.217	0.215	0.217	0.218
0.211	0.211	0.207	0.212	0.200
0.200	0.211	0.218	0.211	0.202
0.199	0.200	0.200	0.201	0.197

d. At depth of 7 mm

0.182	0.186	0.173	0.186	0.176
0.184	0.182	0.179	0.183	0.184
0.175	0.174	0.172	0.170	0.160
0.168	0.175	0.181	0.173	0.163
0.168	0.162	0.162	0.166	0.163

e. At depth of 9 mm

0.158	0.164	0.149	0.163	0.154
0.161	0.159	0.155	0.157	0.161
0.152	0.149	0.149	0.142	0.135
0.145	0.152	0.156	0.147	0.141
0.146	0.140	0.139	0.143	0.140

Table 4. **Above-Lap position (Configuration 1).** The SARs measured for the Wistron NeWeb Model BQ12 802.11a **Auxiliary** Wireless Antenna for the base mode at 5.26 GHz.

1-g SAR = 0.164 W/kg

a. At depth of 1 mm

0.258	0.279	0.287	0.278	0.282
0.263	0.277	0.279	0.272	0.255
0.258	0.282	0.265	0.275	0.271
0.300	0.283	0.290	0.265	0.277
0.278	0.302	0.276	0.277	0.285

b. At depth of 3 mm

0.194	0.213	0.213	0.204	0.204
0.203	0.210	0.210	0.205	0.192
0.205	0.212	0.203	0.202	0.202
0.217	0.209	0.213	0.203	0.203
0.209	0.224	0.207	0.210	0.212

c. At depth of 5 mm

0.143	0.158	0.154	0.145	0.143
0.152	0.155	0.152	0.149	0.141
0.158	0.154	0.152	0.144	0.145
0.151	0.148	0.152	0.152	0.144
0.154	0.160	0.151	0.155	0.156

d. At depth of 7 mm

0.104	0.116	0.109	0.099	0.099
0.112	0.111	0.107	0.106	0.101
0.119	0.110	0.110	0.101	0.102
0.101	0.102	0.105	0.110	0.098
0.112	0.111	0.107	0.111	0.117

e. At depth of 9 mm

0.079	0.085	0.078	0.069	0.072
0.081	0.080	0.073	0.074	0.072
0.088	0.080	0.078	0.072	0.073
0.067	0.070	0.074	0.078	0.068
0.084	0.076	0.076	0.080	0.096

Table 5. **Above-Lap position (Configuration 1).** The SARs measured for the Wistron NeWeb Model BQ12 802.11a **Main** Wireless Antenna for the turbo mode at 5.29 GHz.

1-g SAR = 0.206 W/kg

a. At depth of 1 mm

0.285	0.298	0.298	0.282	0.287
0.316	0.313	0.322	0.318	0.311
0.299	0.301	0.304	0.290	0.306
0.304	0.311	0.297	0.312	0.275
0.304	0.316	0.310	0.300	0.267

b. At depth of 3 mm

0.231	0.241	0.239	0.226	0.231
0.251	0.248	0.256	0.250	0.246
0.239	0.244	0.244	0.241	0.237
0.244	0.246	0.238	0.245	0.224
0.240	0.247	0.249	0.245	0.226

c. At depth of 5 mm

0.188	0.196	0.192	0.182	0.186
0.200	0.197	0.204	0.197	0.195
0.191	0.198	0.196	0.199	0.184
0.196	0.194	0.191	0.192	0.183
0.190	0.193	0.201	0.200	0.192

d. At depth of 7 mm

0.157	0.164	0.157	0.150	0.152
0.163	0.160	0.165	0.159	0.158
0.155	0.163	0.160	0.167	0.147
0.161	0.154	0.156	0.153	0.153
0.154	0.154	0.166	0.165	0.165

e. At depth of 9 mm

0.136	0.143	0.134	0.128	0.130
0.141	0.138	0.140	0.138	0.133
0.133	0.138	0.136	0.142	0.125
0.138	0.128	0.133	0.128	0.133
0.133	0.130	0.143	0.139	0.147

Table 6. **Above-Lap position (Configuration 1).** The SARs measured for the Wistron NeWeb Model BQ12 802.11a **Auxiliary** Wireless Antenna for the turbo mode at 5.29 GHz.

1-g SAR = 0.125 W/kg

a. At depth of 1 mm

0.205	0.210	0.199	0.196	0.195
0.201	0.199	0.199	0.186	0.200
0.217	0.201	0.200	0.201	0.207
0.194	0.207	0.214	0.224	0.202
0.221	0.207	0.216	0.208	0.211

b. At depth of 3 mm

0.156	0.163	0.155	0.150	0.149
0.155	0.155	0.155	0.148	0.154
0.163	0.155	0.156	0.151	0.152
0.154	0.160	0.166	0.169	0.150
0.156	0.156	0.158	0.156	0.161

c. At depth of 5 mm

0.117	0.124	0.119	0.112	0.111
0.117	0.118	0.118	0.117	0.118
0.120	0.117	0.117	0.112	0.108
0.120	0.121	0.126	0.124	0.108
0.105	0.115	0.112	0.115	0.122

d. At depth of 7 mm

0.089	0.093	0.091	0.082	0.082
0.087	0.088	0.088	0.091	0.090
0.088	0.087	0.086	0.081	0.075
0.092	0.090	0.094	0.088	0.076
0.069	0.084	0.077	0.085	0.095

e. At depth of 9 mm

0.071	0.071	0.070	0.061	0.062
0.066	0.066	0.066	0.071	0.071
0.066	0.066	0.061	0.061	0.054
0.070	0.068	0.070	0.063	0.054
0.048	0.063	0.054	0.067	0.079

Table 7. **Edge-On position (Configuration 2).** The SARs measured for the Wistron NeWeb Model BQ12 802.11a **Main** Wireless Antenna for the base mode at 5.26 GHz.

1-g SAR = 0.699 W/kg

a. At depth of 1 mm

1.314	1.335	1.285	1.225	1.149
1.398	1.406	1.378	1.327	1.199
1.397	1.435	1.427	1.356	1.233
1.311	1.386	1.350	1.332	1.213
1.199	1.283	1.259	1.188	1.131

b. At depth of 3 mm

0.930	0.943	0.914	0.878	0.823
0.983	0.992	0.975	0.938	0.855
0.979	1.010	1.009	0.960	0.881
0.932	0.977	0.959	0.943	0.867
0.858	0.904	0.893	0.853	0.809

c. At depth of 5 mm

0.624	0.631	0.619	0.601	0.564
0.655	0.663	0.655	0.628	0.580
0.648	0.674	0.677	0.645	0.600
0.629	0.652	0.647	0.634	0.591
0.585	0.604	0.602	0.585	0.554

d. At depth of 7 mm

0.398	0.400	0.399	0.394	0.370
0.412	0.419	0.415	0.398	0.374
0.405	0.427	0.431	0.412	0.390
0.404	0.411	0.415	0.403	0.385
0.380	0.382	0.386	0.385	0.365

e. At depth of 9 mm

0.251	0.251	0.255	0.256	0.242
0.255	0.259	0.257	0.247	0.237
0.249	0.268	0.269	0.261	0.251
0.256	0.254	0.262	0.252	0.248
0.243	0.239	0.244	0.252	0.243

Table 8. **Edge-On position (Configuration 2).** The SARs measured for the Wistron NeWeb Model BQ12 802.11a **Auxiliary** Wireless Antenna for the base mode at 5.26 GHz.

1-g SAR = 0.909 W/kg

a. At depth of 1 mm

1.507	1.632	1.725	1.770	1.770
1.671	1.791	1.887	1.926	1.887
1.750	1.894	1.939	1.961	1.904
1.754	1.867	1.904	1.914	1.817
1.648	1.776	1.792	1.762	1.679

B. At depth of 3 mm

1.034	1.113	1.176	1.197	1.204
1.150	1.226	1.284	1.309	1.284
1.205	1.288	1.319	1.337	1.297
1.207	1.280	1.305	1.306	1.242
1.140	1.218	1.221	1.206	1.143

c. At depth of 5 mm

0.664	0.710	0.747	0.752	0.764
0.742	0.785	0.814	0.828	0.814
0.778	0.816	0.836	0.850	0.824
0.778	0.821	0.837	0.832	0.792
0.741	0.782	0.778	0.772	0.729

d. At depth of 7 mm

0.398	0.421	0.439	0.436	0.450
0.447	0.468	0.477	0.485	0.478
0.470	0.477	0.489	0.502	0.485
0.466	0.488	0.500	0.492	0.470
0.450	0.468	0.462	0.460	0.435

e. At depth of 9 mm

0.235	0.248	0.252	0.249	0.261
0.265	0.275	0.273	0.278	0.276
0.279	0.271	0.279	0.291	0.280
0.272	0.281	0.296	0.286	0.274
0.268	0.276	0.273	0.270	0.263

Table 9. **Edge-On position (Configuration 2).** The SARs measured for the Wistron NeWeb Model BQ12 802.11a **Main** Wireless Antenna for the turbo mode at 5.29 GHz.

1-g SAR = 0.613 W/kg

a. At depth of 1 mm

1.085	1.109	1.110	1.086	1.014
1.156	1.181	1.211	1.158	1.104
1.175	1.211	1.240	1.188	1.138
1.105	1.156	1.201	1.182	1.117
1.022	1.091	1.088	1.075	1.031

b. At depth of 3 mm

0.774	0.793	0.789	0.771	0.731
0.825	0.846	0.859	0.825	0.791
0.834	0.861	0.875	0.848	0.813
0.791	0.829	0.847	0.839	0.798
0.730	0.770	0.778	0.768	0.744

c. At depth of 5 mm

0.528	0.542	0.533	0.522	0.505
0.560	0.578	0.579	0.561	0.541
0.562	0.584	0.585	0.577	0.553
0.541	0.567	0.567	0.567	0.544
0.499	0.517	0.531	0.524	0.515

d. At depth of 7 mm

0.346	0.355	0.344	0.339	0.336
0.362	0.377	0.370	0.363	0.355
0.360	0.377	0.370	0.375	0.360
0.354	0.371	0.362	0.363	0.353
0.327	0.331	0.346	0.342	0.344

e. At depth of 9 mm

0.229	0.232	0.222	0.221	0.224
0.230	0.242	0.233	0.233	0.233
0.227	0.241	0.231	0.242	0.232
0.231	0.241	0.232	0.230	0.228
0.214	0.213	0.223	0.222	0.230

Table 10. **Edge-On position (Configuration 2).** The SARs measured for the Wistron NeWeb Model BQ12 802.11a **Auxiliary** Wireless Antenna for the turbo mode at 5.29 GHz.

1-g SAR = 0.597 W/kg

a. At depth of 1 mm

1.016	1.101	1.191	1.208	1.175
1.090	1.175	1.277	1.291	1.270
1.148	1.227	1.308	1.328	1.295
1.124	1.227	1.272	1.290	1.263
1.079	1.163	1.201	1.217	1.162

b. At depth of 3 mm

0.688	0.745	0.801	0.805	0.787
0.738	0.790	0.852	0.873	0.857
0.776	0.827	0.879	0.889	0.870
0.767	0.832	0.863	0.869	0.850
0.735	0.787	0.818	0.828	0.798

c. At depth of 5 mm

0.433	0.468	0.500	0.493	0.486
0.464	0.492	0.525	0.547	0.536
0.487	0.516	0.545	0.549	0.541
0.490	0.524	0.544	0.542	0.529
0.466	0.497	0.520	0.526	0.516

d. At depth of 7 mm

0.252	0.271	0.287	0.274	0.272
0.268	0.281	0.295	0.314	0.309
0.279	0.293	0.306	0.308	0.309
0.292	0.303	0.316	0.309	0.301
0.272	0.293	0.309	0.312	0.317

e. At depth of 9 mm

0.144	0.154	0.162	0.146	0.144
0.150	0.157	0.162	0.174	0.174
0.153	0.160	0.163	0.165	0.173
0.173	0.171	0.179	0.171	0.166
0.155	0.176	0.184	0.185	0.200

Table 11. The peak 1-g SARs measured for the Wistron NeWeb Corporation 802.11a Wireless Antennas built into Model BQ12 Notebook PC (FCC ID# NKRBQ12AB).

			1-g SAR in W/kg	
PC position relative to the flat phantom	Spacing to the bottom of the phantom	Antenna	5.26 GHz base mode	5.29 GHz turbo mode
Configuration 1 – **"Above-Lap" position**; bottom of PC pressed against bottom of the flat phantom	0 cm	Main Auxiliary	0.223 0.164	0.206 0.125
Configuration 2 – **"Edge-On"** placement; right or left edge of the PC at 90° and at a distance of 1.5 cm from the base of the phantom (see Figs. 4a, 4b)	1.5 cm	Main Auxiliary	0.699 0.909	0.613 0.597

a. Top cover closed.

Fig. 1. Photograph of the Model BQ12 Notebook Computer with built-in Wistron Model EM-500 AG 802.11 a/b/g Mini PCI Card.

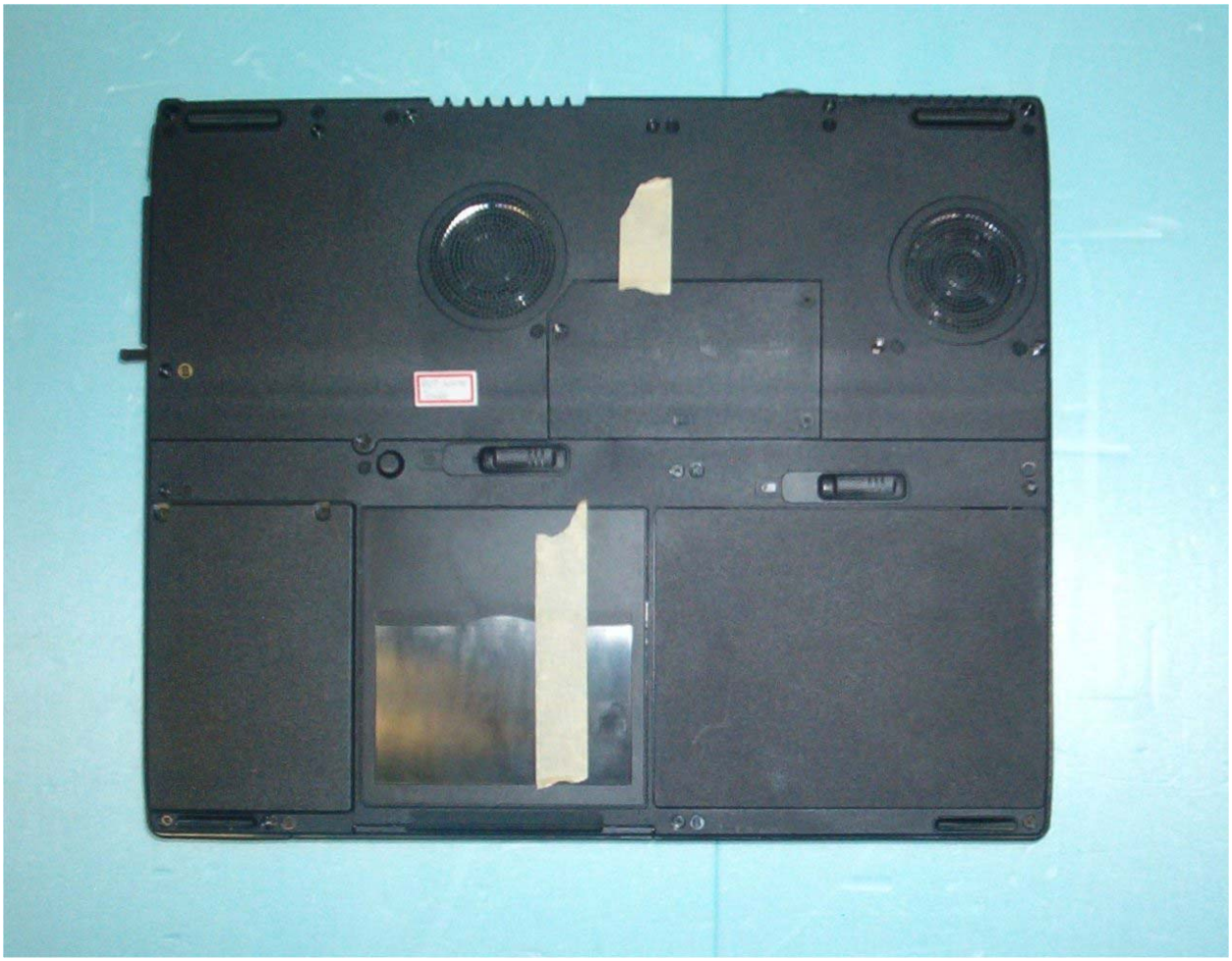

b. View from bottom side of the laptop computer.

Fig. 1. Photograph of the Model BQ12 Notebook Computer with built-in Wistron Model EM-500 AG 802.11 a/b/g Mini PCI Card.

c. Top cover with screen open.

Fig. 1. Photograph of the Model BQ12 Notebook Computer with built-in Wistron Model EM-500 AG 802.11 a/b/g Mini PCI Card.

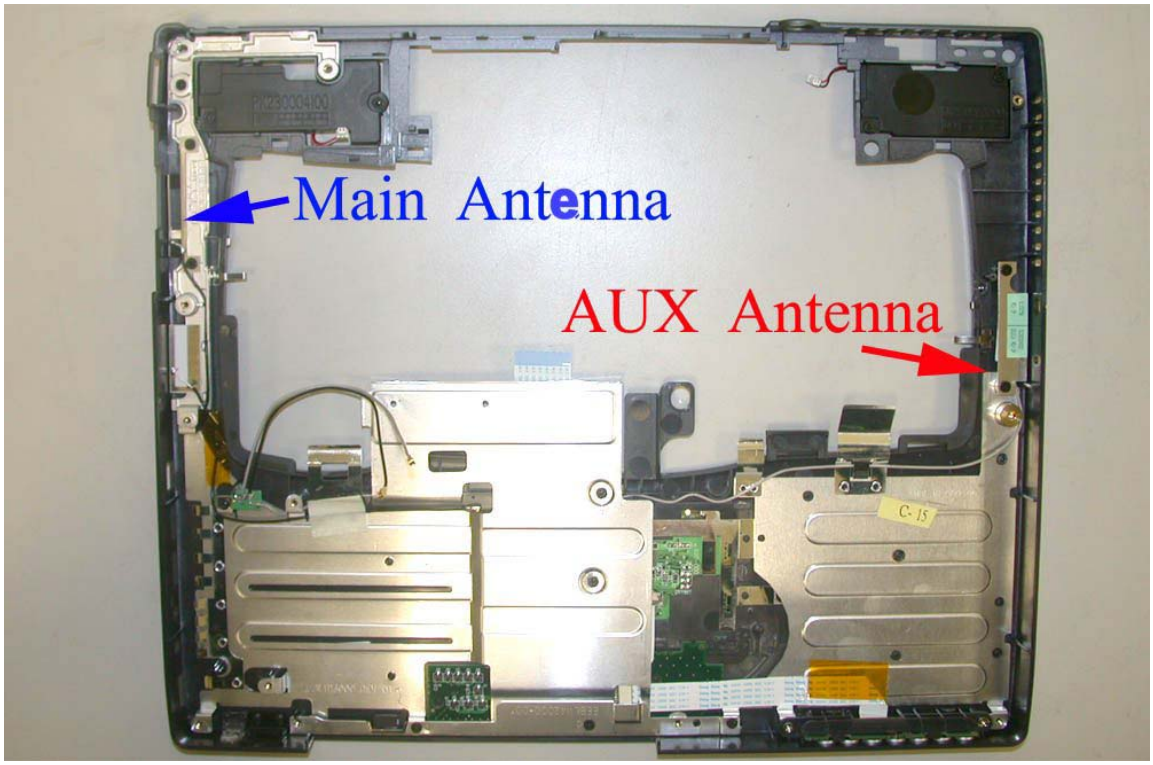

Fig. 2. Photograph of the base of the Model BQ12 Notebook Computer showing the relative locations of the Wistron 802.11a Wireless Antennas marked as "Main" and "Aux" antennas.

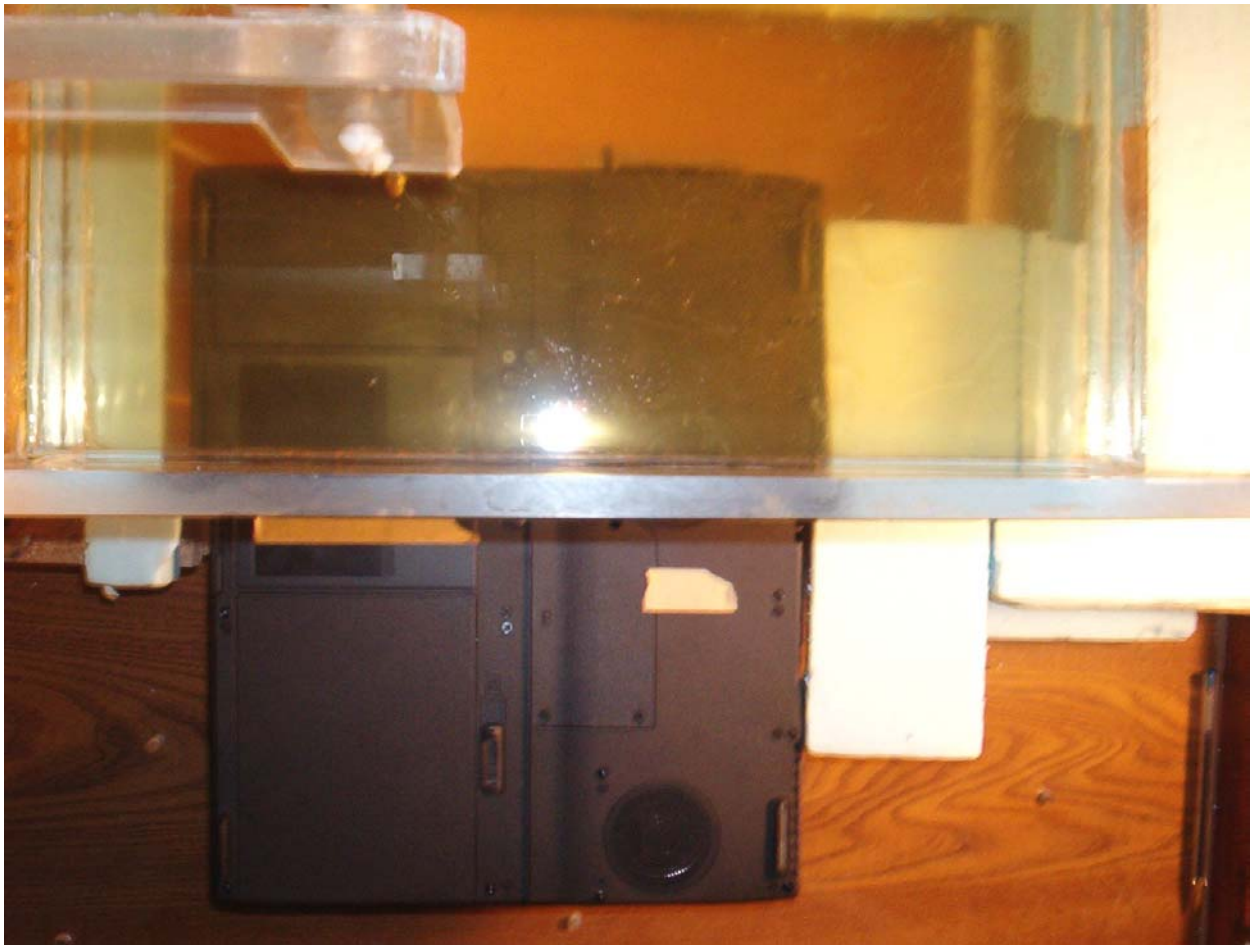

a. The right edge with "Main " antenna pressed against the planar phantom.

Fig. 3. Photograph of the bottom of the Model BQ12 Notebook Computer with built-in Wistron 802.11a Wireless Antennas pressed against the base of the planar phantom. This is **Configuration 1 – Laptop position** for SAR testing.

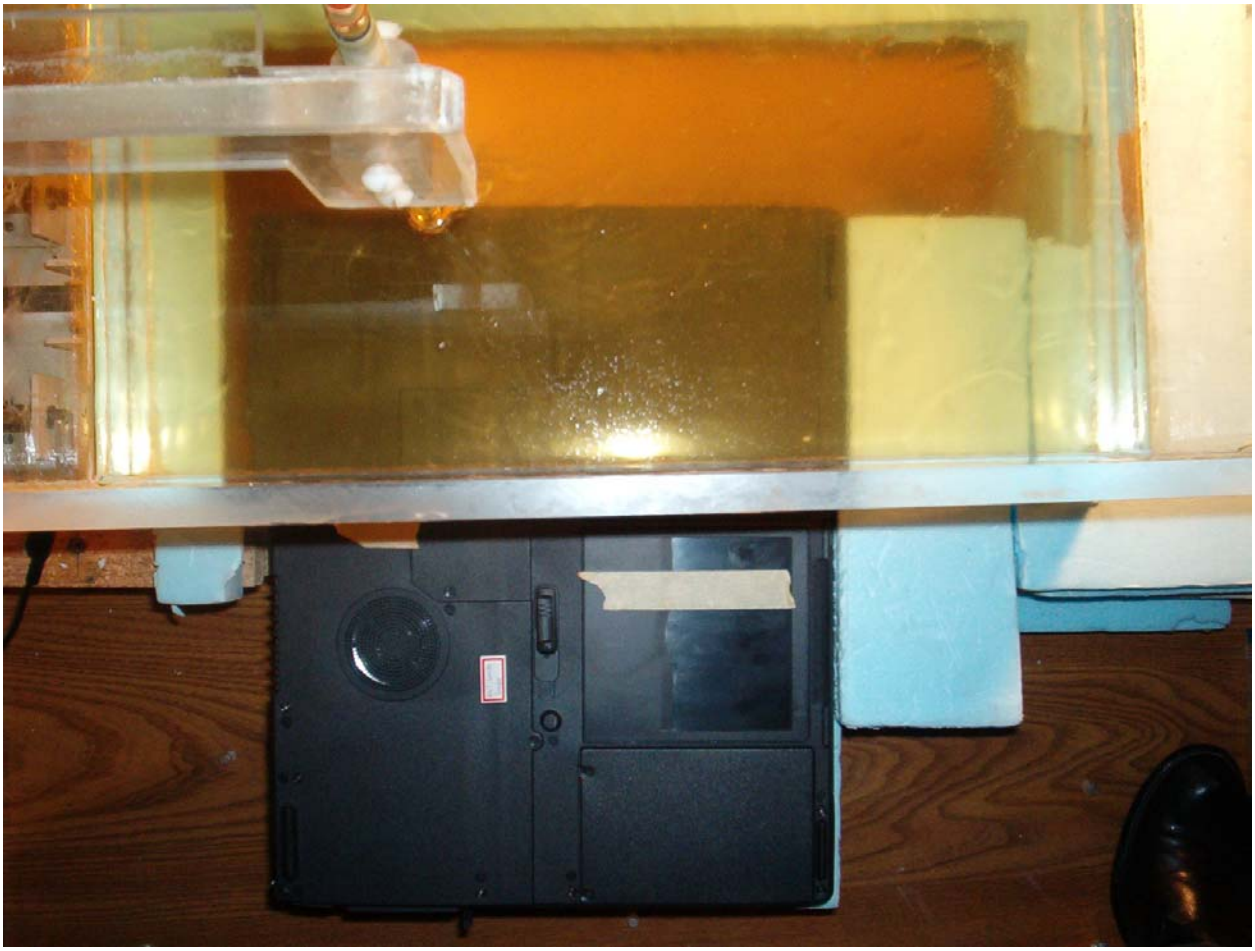

b. The left edge with "Aux" (auxiliary) antenna pressed against the planar phantom.

Fig. 3. Photograph of the bottom of the Model BQ12 Notebook Computer with built-in Wistron 802.11a Wireless Antennas pressed against the base of the planar phantom. This is **Configuration 1 – Laptop position** for SAR testing.

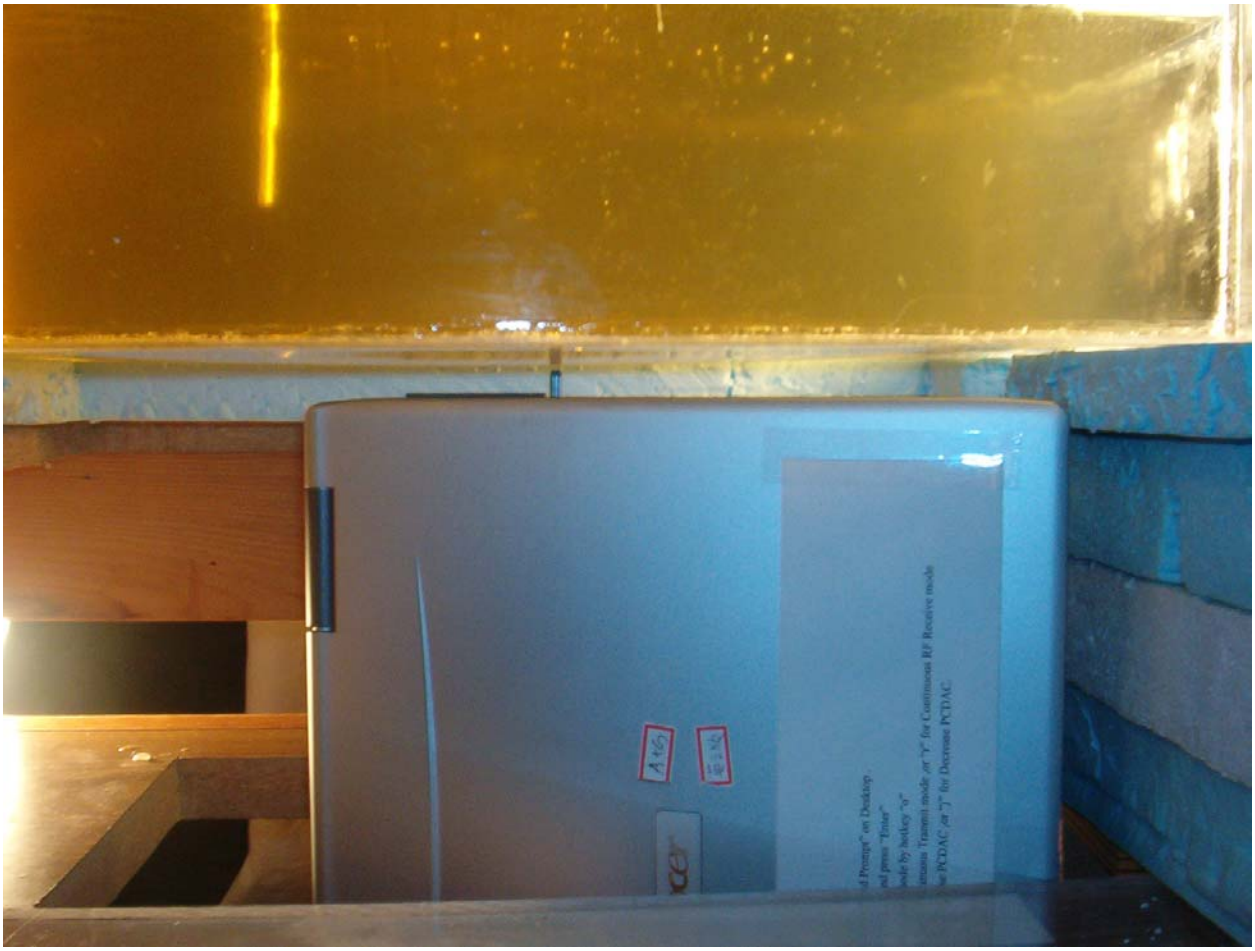

a1. **Side view**. The right edge with "Main" antenna at a distance of 1.5 cm from the bottom of the planar phantom.

Fig. 4. Photograph of the Model BQ12 Notebook Computer with edge of the PC at 90° at a distance of 1.5 cm from the base of the planar phantom. This is **Configuration 2** for SAR Testing and represents the case of a bystander at a distance of 1.5 cm from the side of the laptop computer.

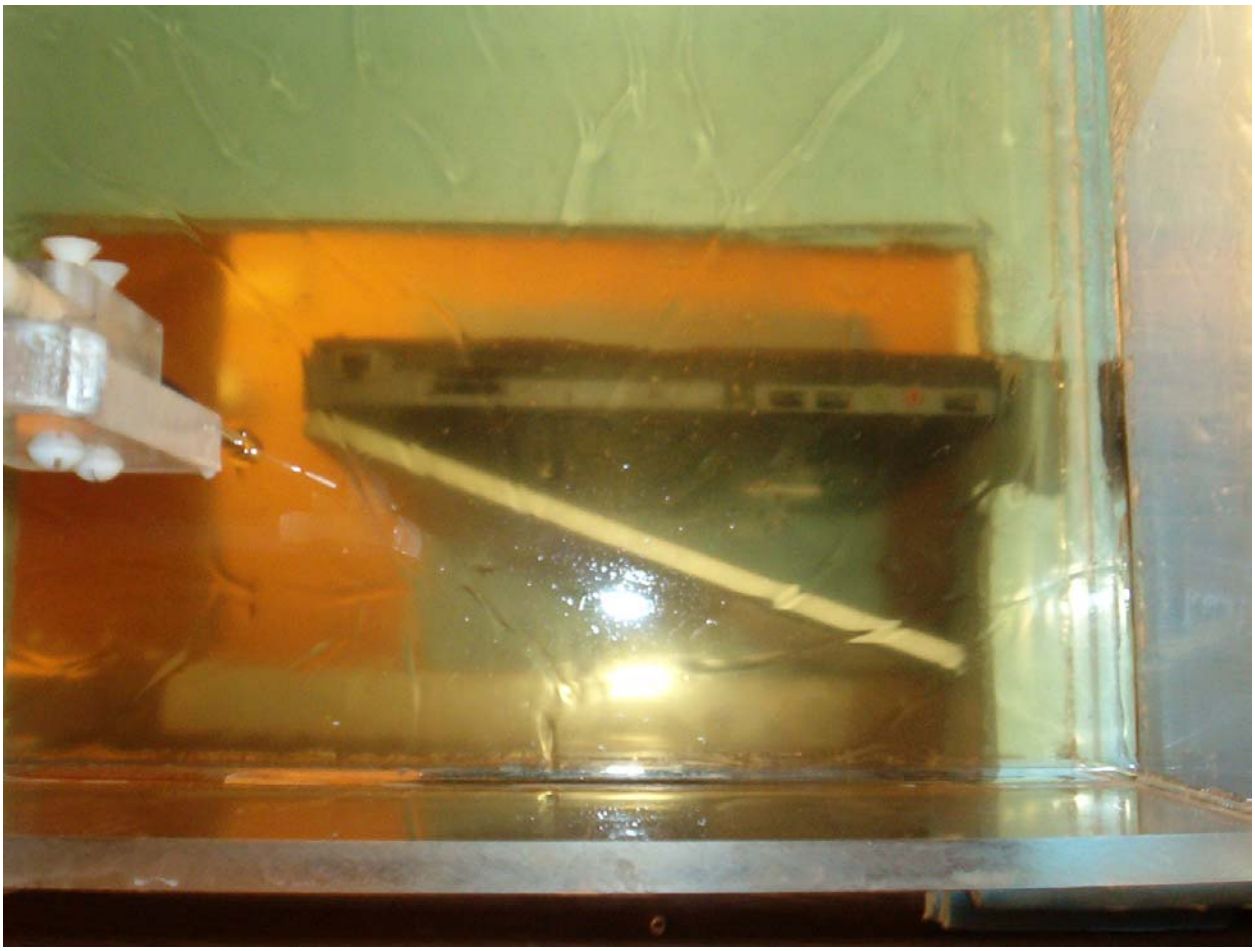

a2. **Top view**. The right edge with "Main" antenna at a distance of 1.5 cm from the bottom of the planar phantom.

Fig. 4. Photograph of the Model BQ12 Notebook Computer with edge of the PC at 90° at a distance of 1.5 cm from the base of the planar phantom. This is **Configuration 2** for SAR Testing and represents the case of a bystander at a distance of 1.5 cm from the side of the laptop computer.

b1. **Side view**. The left edge with "Aux" antenna at a distance of 1.5 cm from the bottom of the planar phantom.

Fig. 4. Photograph of the Model BQ12 Notebook Computer with edge of the PC at 90° at a distance of 1.5 cm from the base of the planar phantom. This is **Configuration 2** for SAR Testing and represents the case of a bystander at a distance of 1.5 cm from the side of the laptop computer.

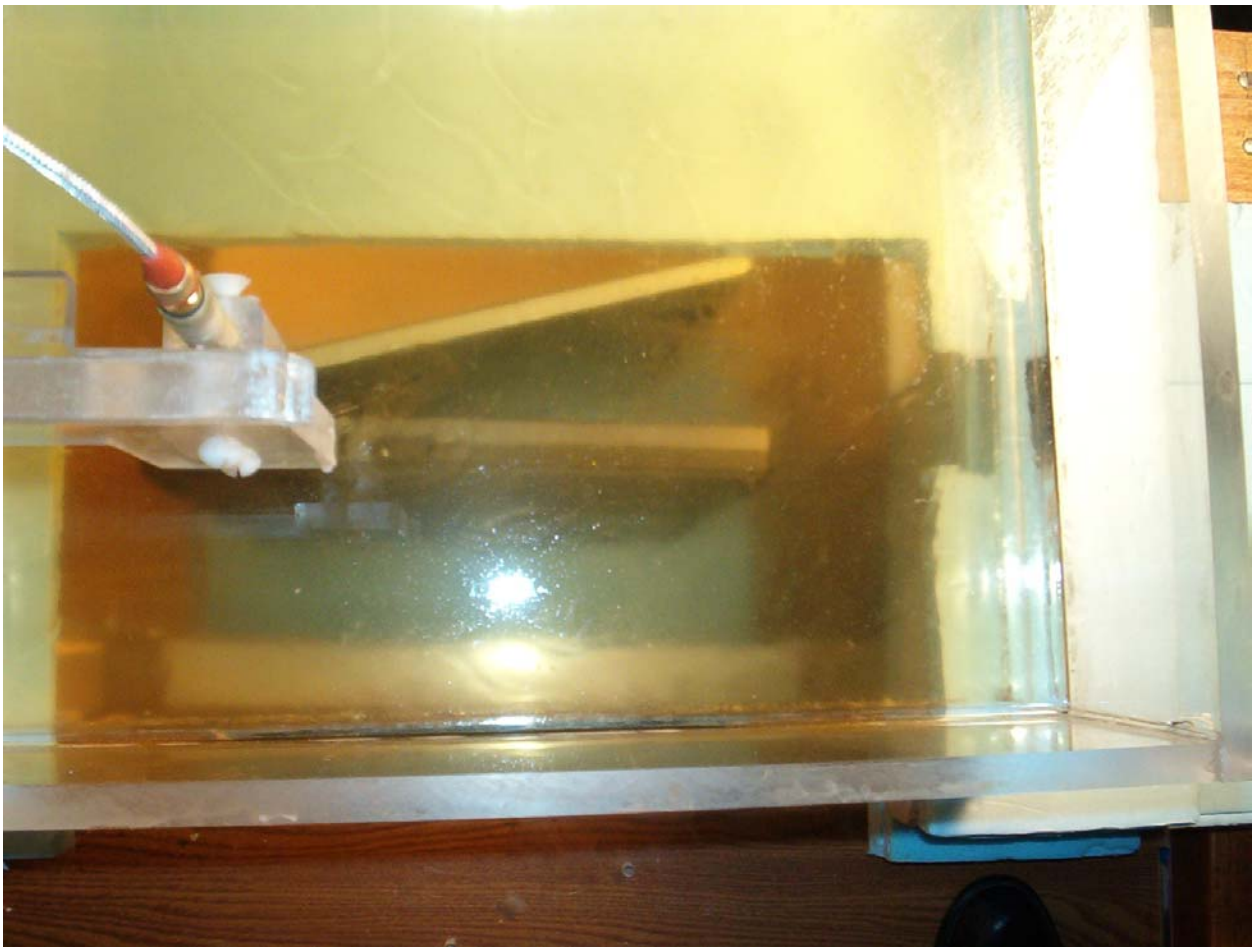

b2. **Top view**. The left edge with "Aux" antenna at a distance of 1.5 cm from the bottom of the planar phantom.

Fig. 4. Photograph of the Model BQ12 Notebook Computer with edge of the PC at 90° at a distance of 1.5 cm from the base of the planar phantom. This is **Configuration 2** for SAR Testing and represents the case of a bystander at a distance of 1.5 cm from the side of the laptop computer.

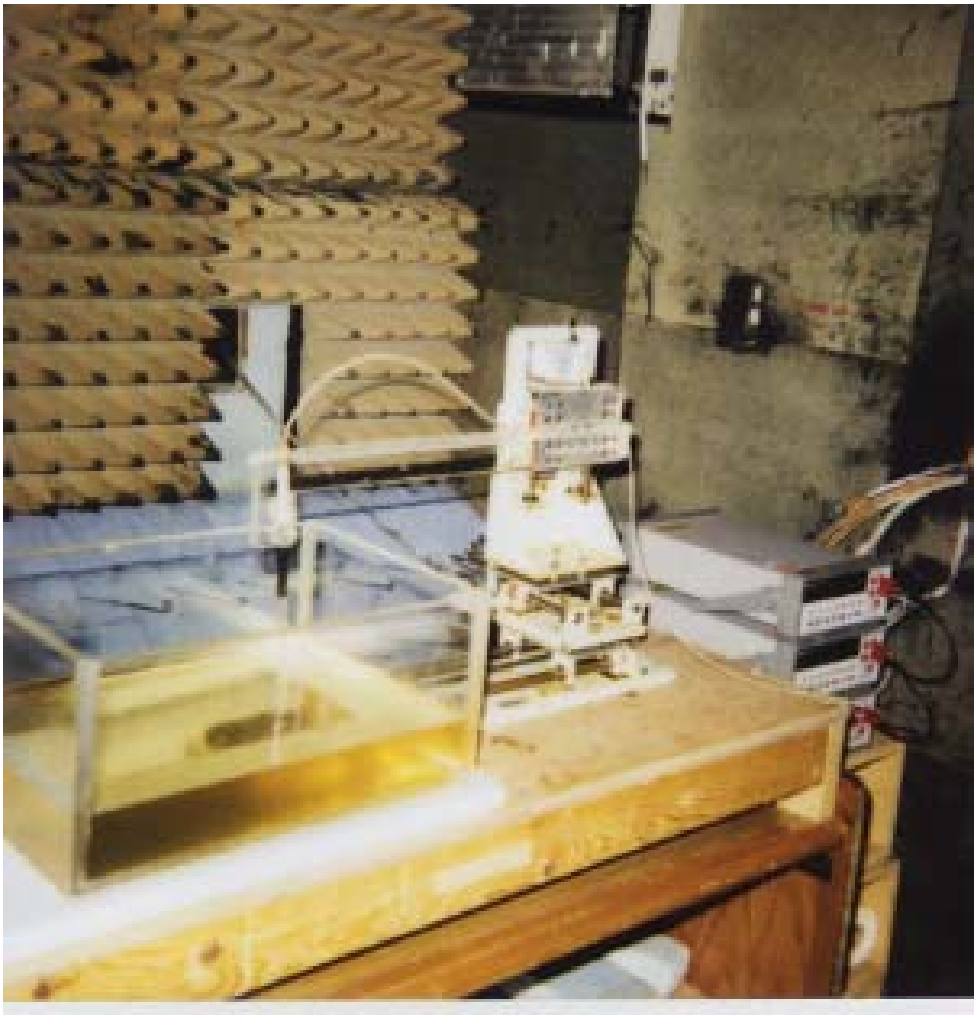

Fig. 5. Photograph of the three-dimensional stepper-motor-controlled SAR measurement system using a planar phantom (see Figs. 3 and 4 for a detailed examination of the placement of Wistron Model BQ12 Notebook Computer with Wistron 802.11a Wireless Antennas relative to this phantom).

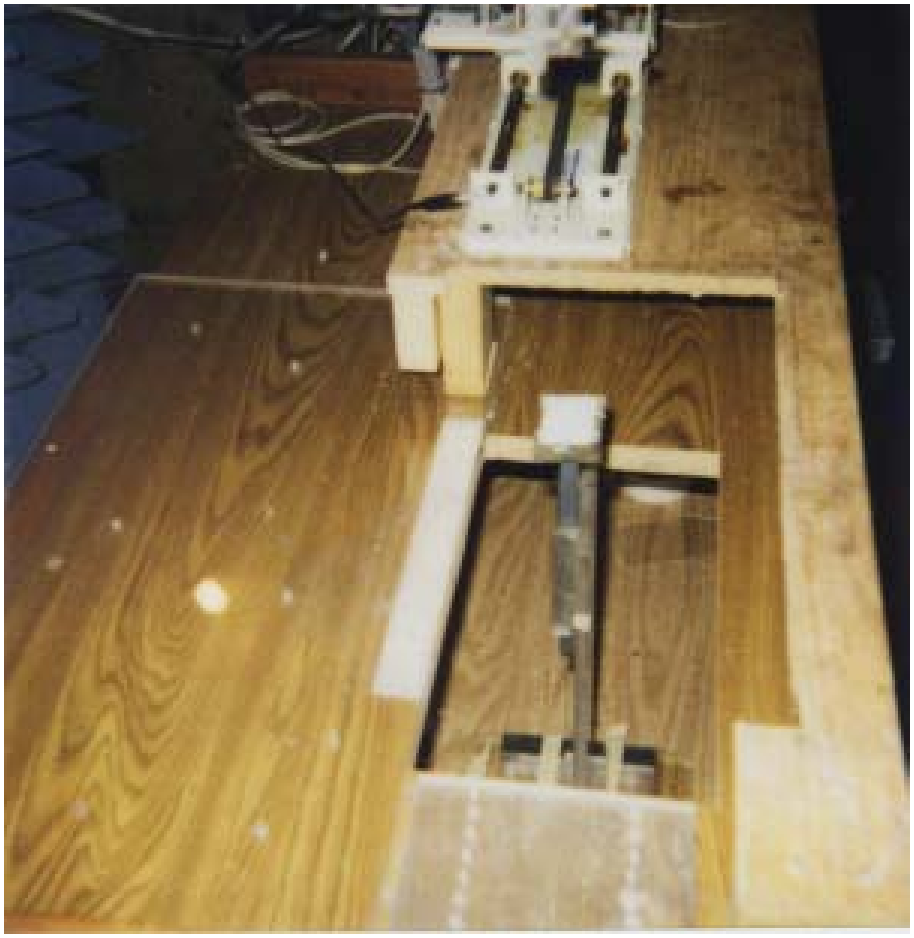

Fig. 6. The plastic holder used to support the portable PC with the Wistron 802.11a Wireless Antennas (shown in Figs. 1, 2).

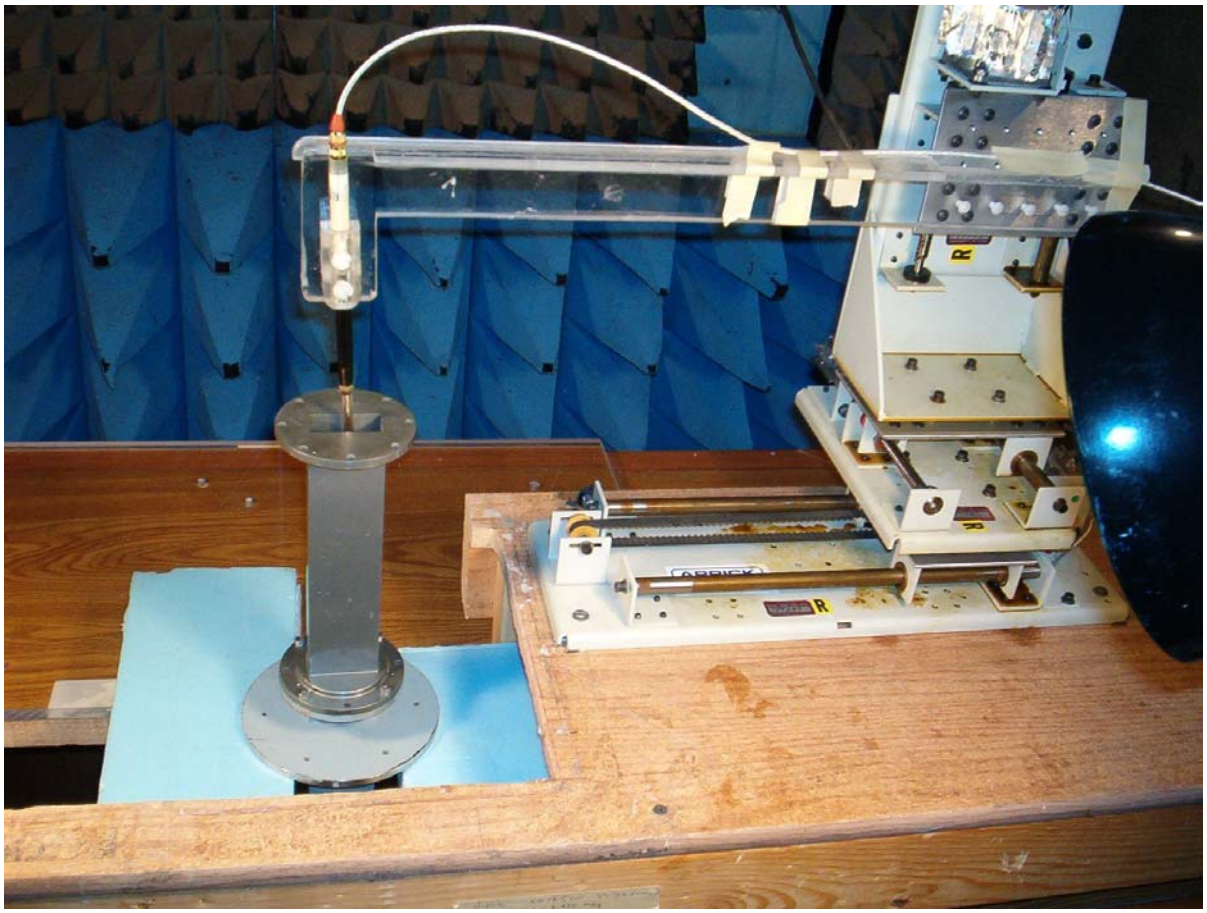

Fig. 7a. A photograph of the waveguide setup used for calibration of the Narda Model 8021 E-field probe in the frequency band 5.2-5.8 GHz.

Fig. 7b. Photograph of the waveguide setup showing also the coax to waveguide coupler at the bottom used to feed power to the vertical waveguide containing the tissue-simulant fluid.

Fig. 8. Photograph of the Narda Model 8021 Broadband Electric Field Probe used for SAR measurements.

Fig. 9. Photograph of the half-wave dipole at 1900 MHz used for system verification.

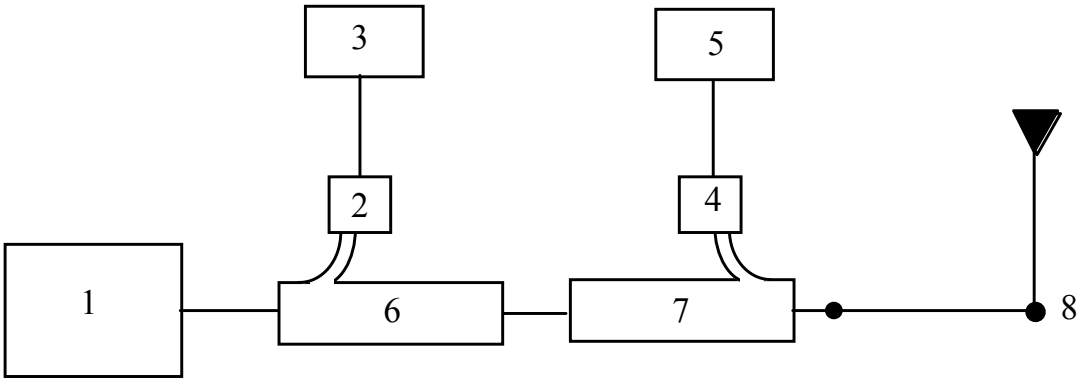

1. RF generator, MCL Model 15222 with Model 6051 plug-in (1000-2000 MHz).
2. HP Model 8481A power sensor.
3. HP Model 436A power meter.
4. HP Model 8482A power sensor.
5. HP Model 436A power meter.
6. Narda Model 3042B-30, 30 dB coaxial directional coupler.
7. Narda Model 3042-10, 10 dB coaxial directional coupler.
8. Reference dipole antenna.

Fig. 10. The microwave circuit arrangement used for SAR system verification.

Fig. 11. Photograph of the Hewlett Packard Model 85070B Dielectric Probe. This is an open-circuited coaxial line probe.

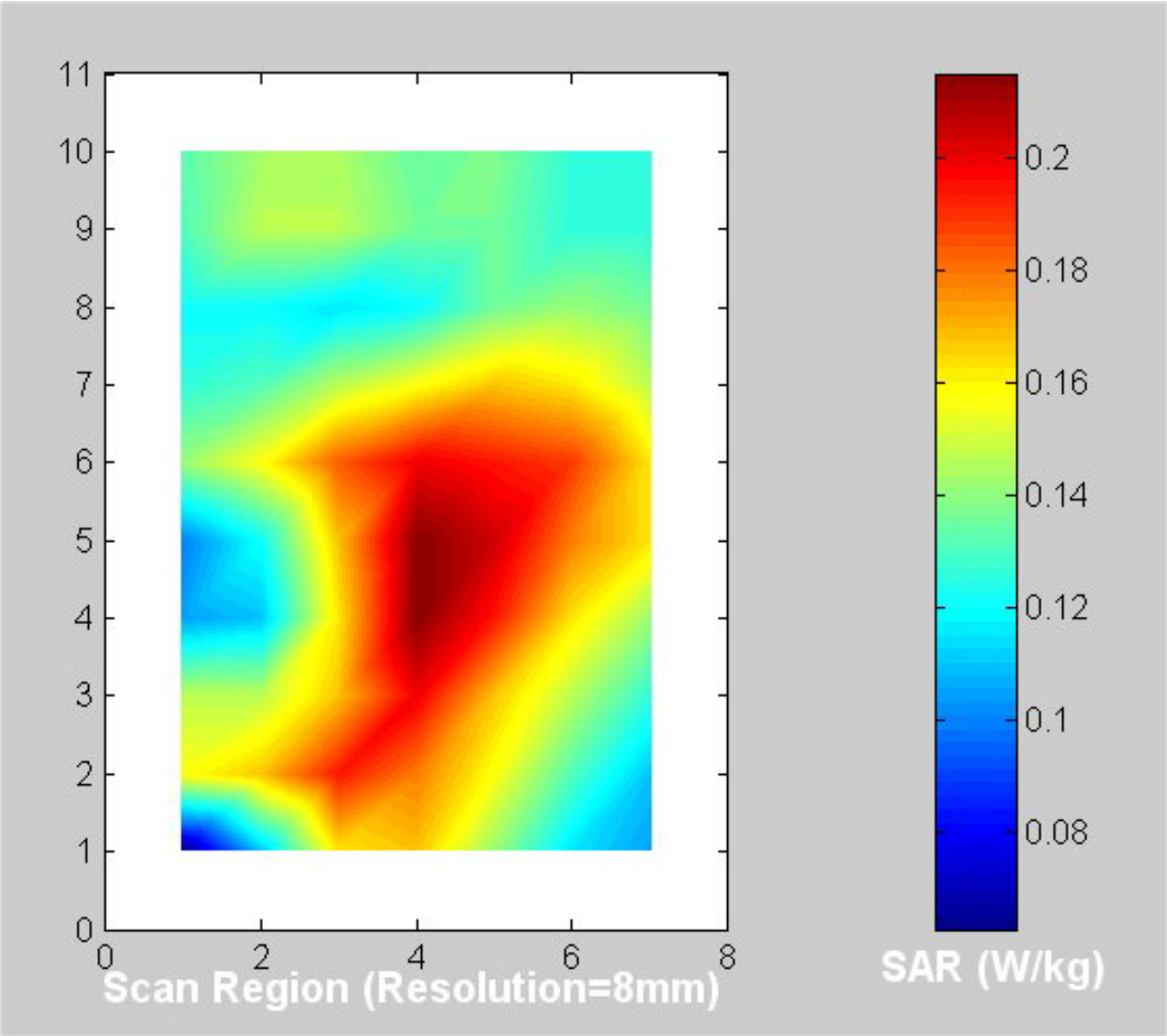

a. 5.26 GHz base mode – Main antenna (see Table 3 for the peak 1-g SAR).

Fig. 12. Coarse scans for the SAR measurements for the **Above-Lap** position of the PC relative to the flat phantom (**Configuration 1,** see Fig. 3). The base of the right or left sides of the PC with Main or Auxiliary 802.11a antennas, respectively, was placed pressed against the bottom of the flat phantom.

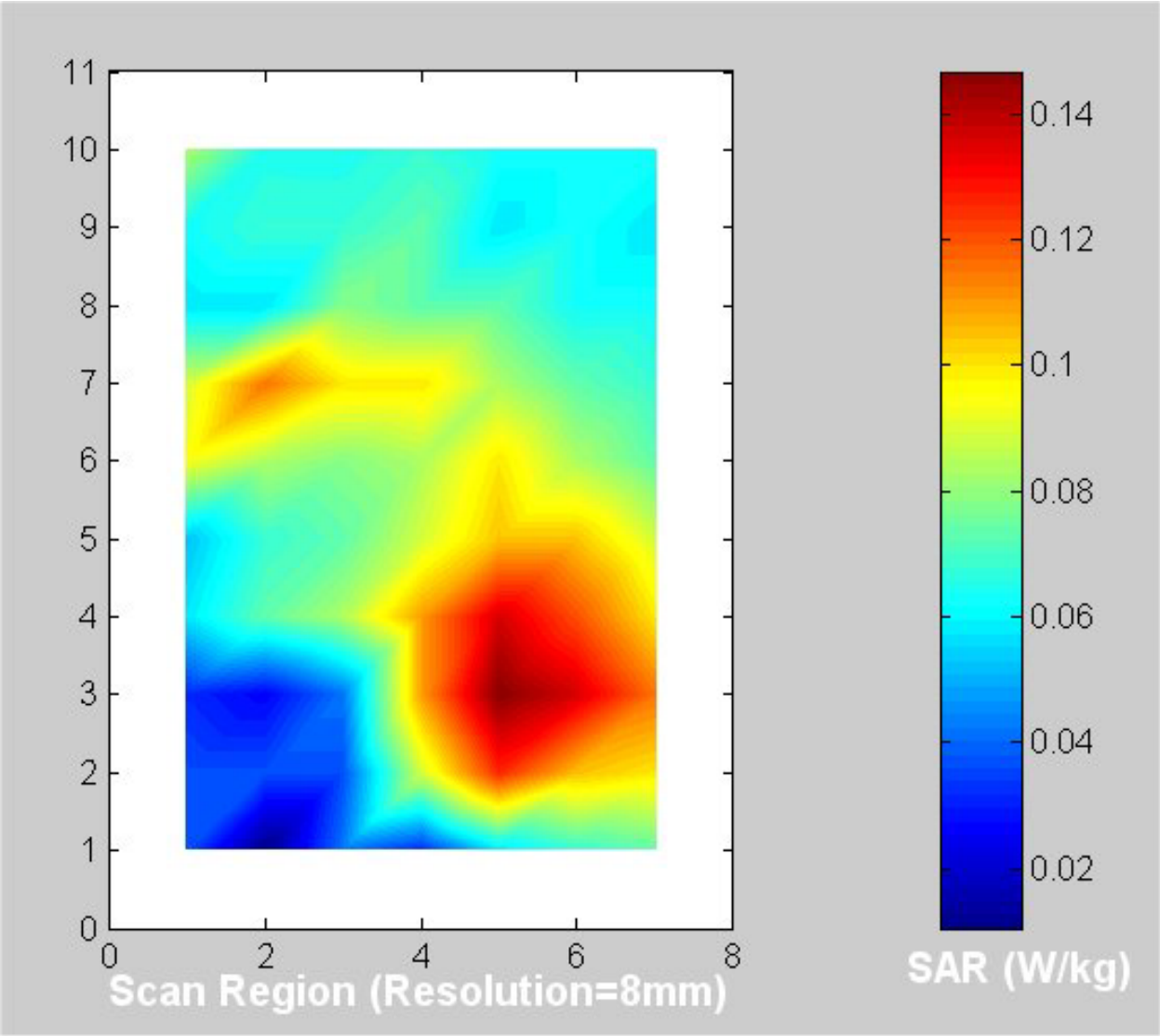

b. 5.26 GHz base mode – Auxiliary antenna (see Table 4 for the peak 1-g SAR).

Fig. 12. Coarse scans for the SAR measurements for the **Above-Lap** position of the PC relative to the flat phantom (**Configuration 1,** see Fig. 3). The base of the right or left sides of the PC with Main or Auxiliary 802.11a antennas, respectively, was placed pressed against the bottom of the flat phantom.

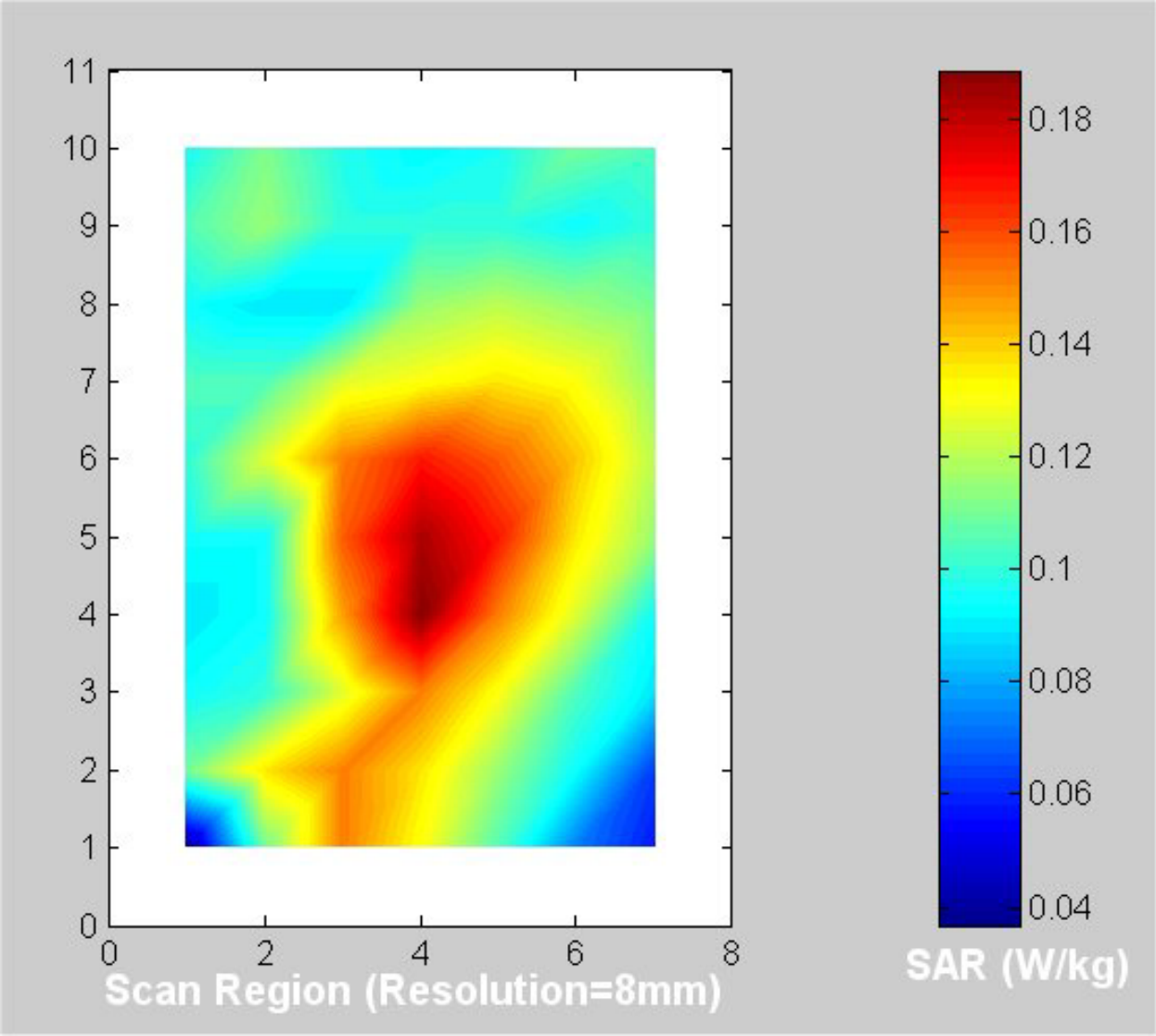

c. 5.29 GHz turbo mode – Main antenna (see Table 5 for the peak 1-g SAR).

Fig. 12. Coarse scans for the SAR measurements for the **Above-Lap** position of the PC relative to the flat phantom (**Configuration 1,** see Fig. 3). The base of the right or left sides of the PC with Main or Auxiliary 802.11a antennas, respectively, was placed pressed against the bottom of the flat phantom.

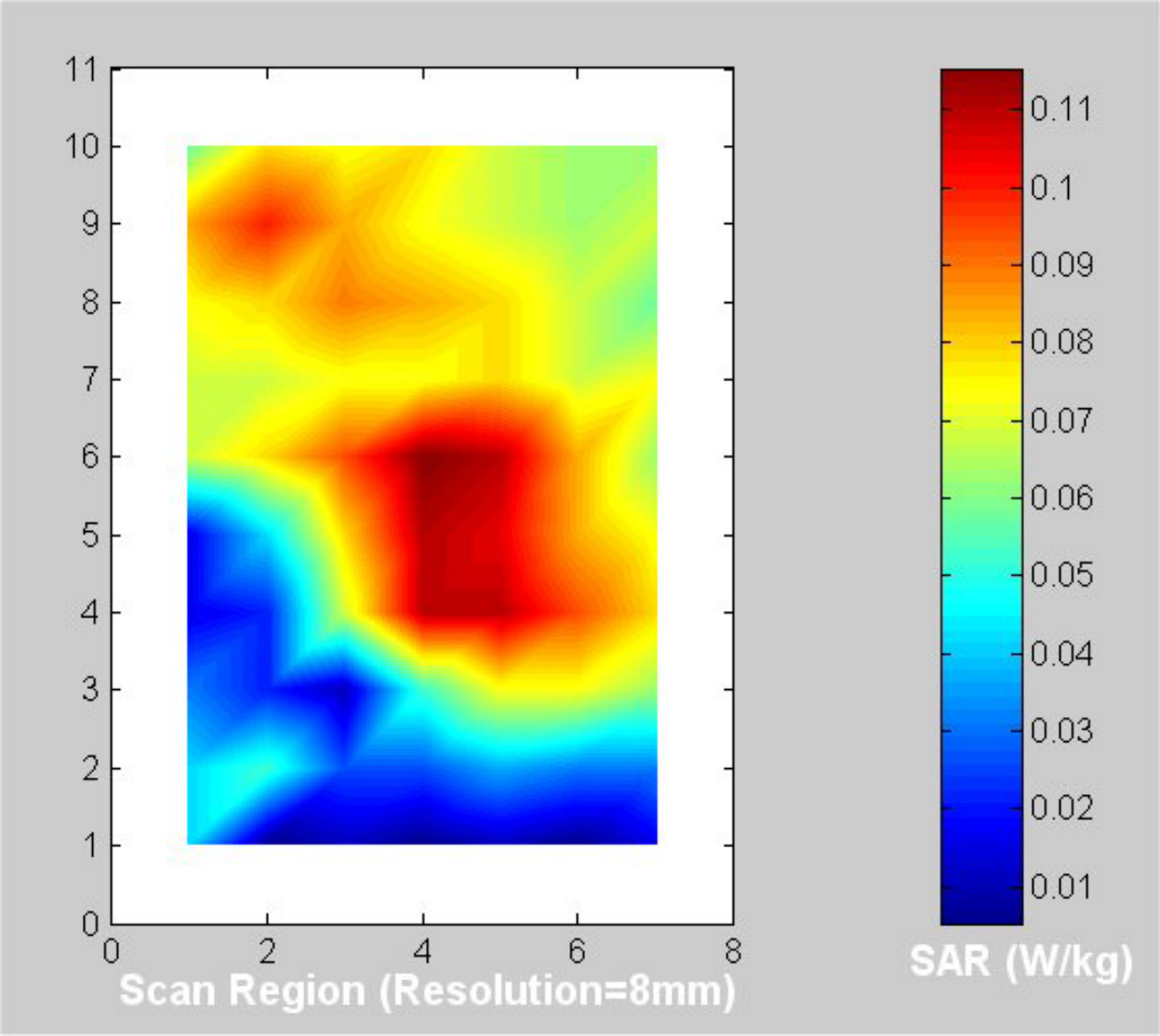

d. 5.29 GHz turbo mode – Auxiliary antenna (see Table 6 for the peak 1-g SAR).

Fig. 12. Coarse scans for the SAR measurements for the **Above-Lap** position of the PC relative to the flat phantom (**Configuration 1,** see Fig. 3). The base of the right or left sides of the PC with Main or Auxiliary 802.11a antennas, respectively, was placed pressed against the bottom of the flat phantom.

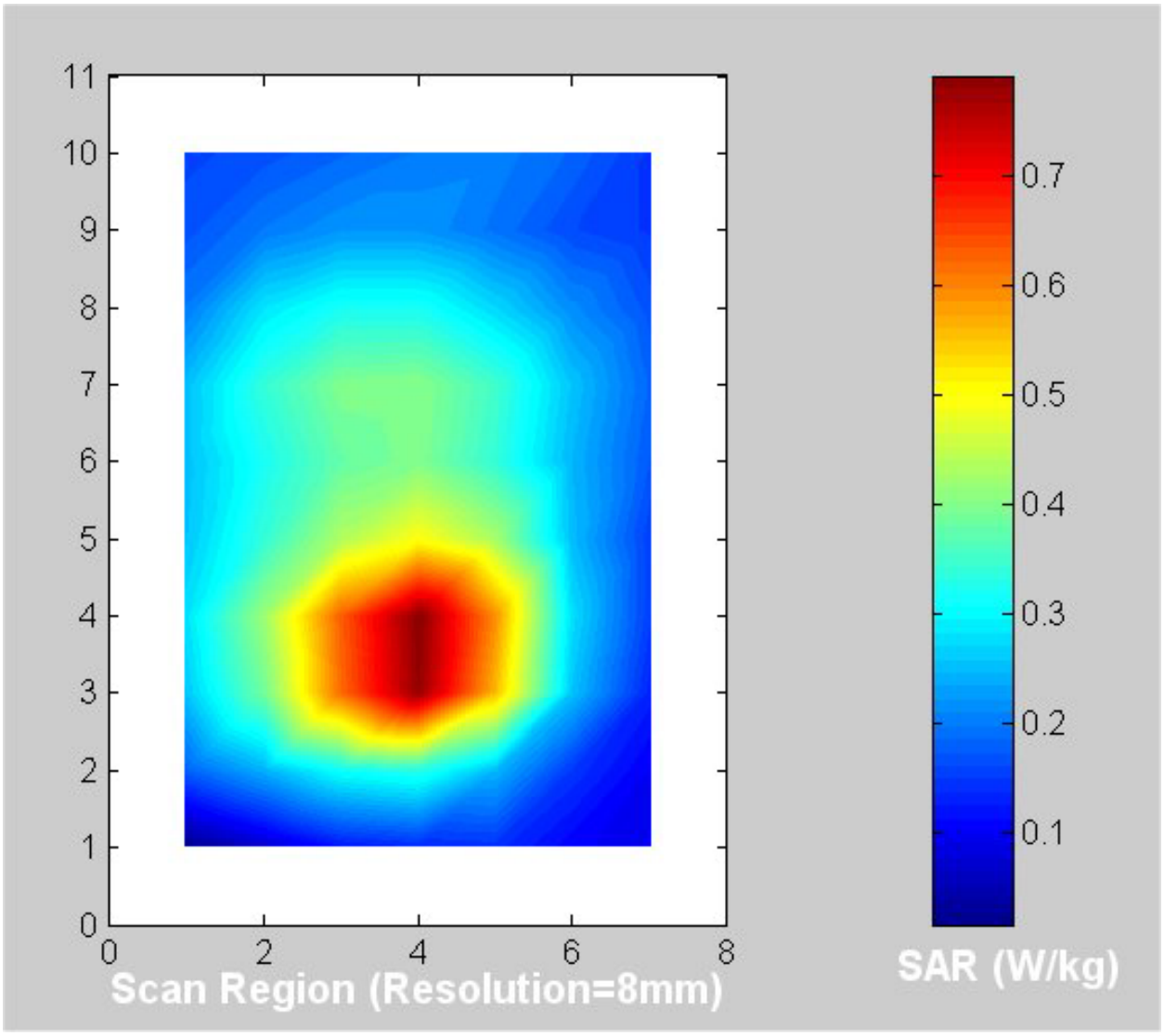

a. 5.26 GHz base mode – Main antenna (see Table 7 for the peak 1-g SAR).

Fig. 13. Coarse scans for the SAR measurements for the **Edge-On position** of the PC relative to the flat phantom **(Configuration 2,** see Fig. 4**)**. The right or the left edge of the PC with the 802.11a Main or Auxiliary antennas, respectively, was placed at 90° at a distance of 1.5 cm from the bottom of the flat phantom.

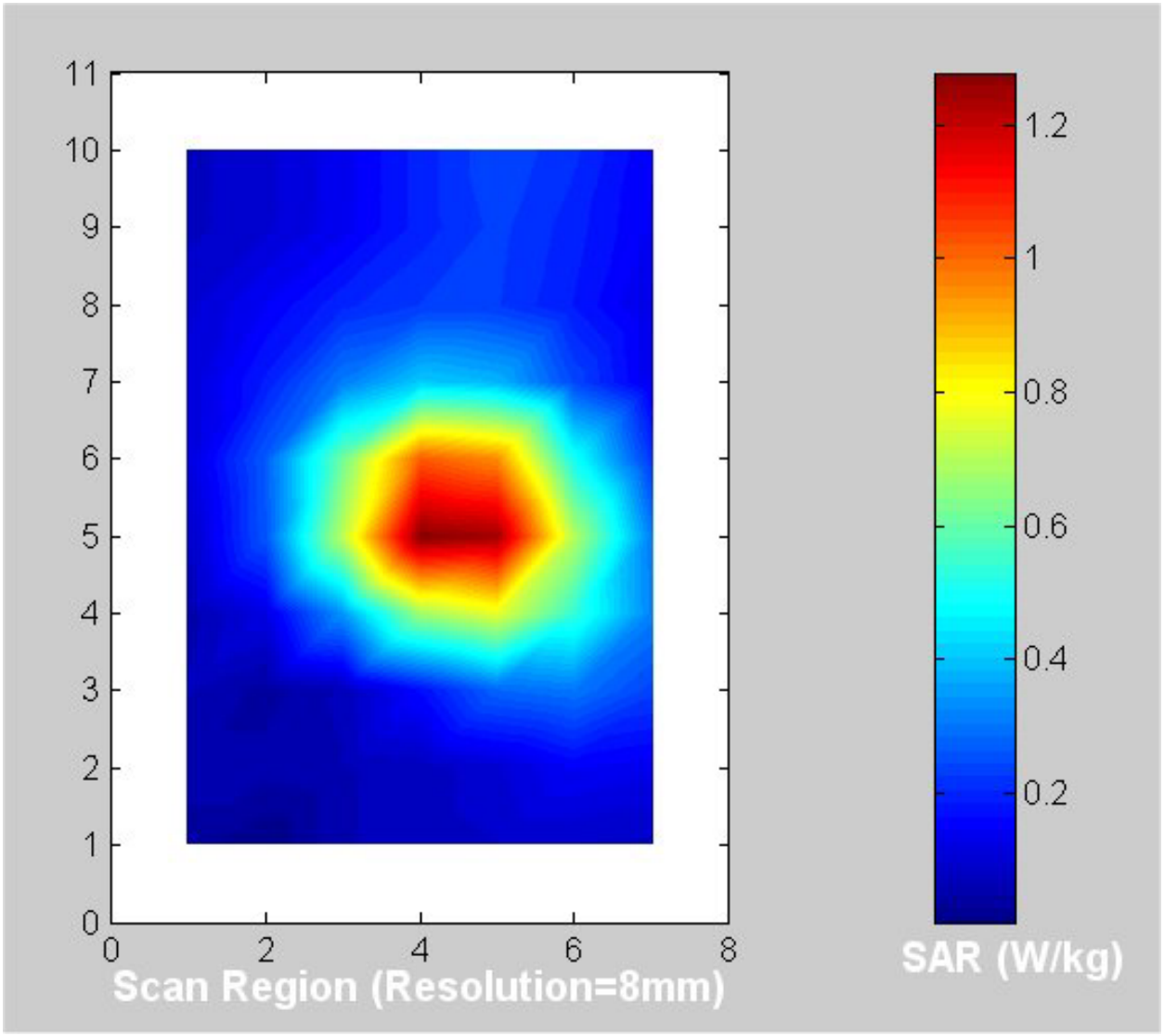

b. 5.26 GHz base mode – Auxiliary antenna (see Table 8 for the peak 1-g SAR).

Fig. 13. Coarse scans for the SAR measurements for the **Edge-On position** of the PC relative to the flat phantom **(Configuration 2,** see Fig. 4**)**. The right or the left edge of the PC with the 802.11a Main or Auxiliary antennas, respectively, was placed at 90° at a distance of 1.5 cm from the bottom of the flat phantom.

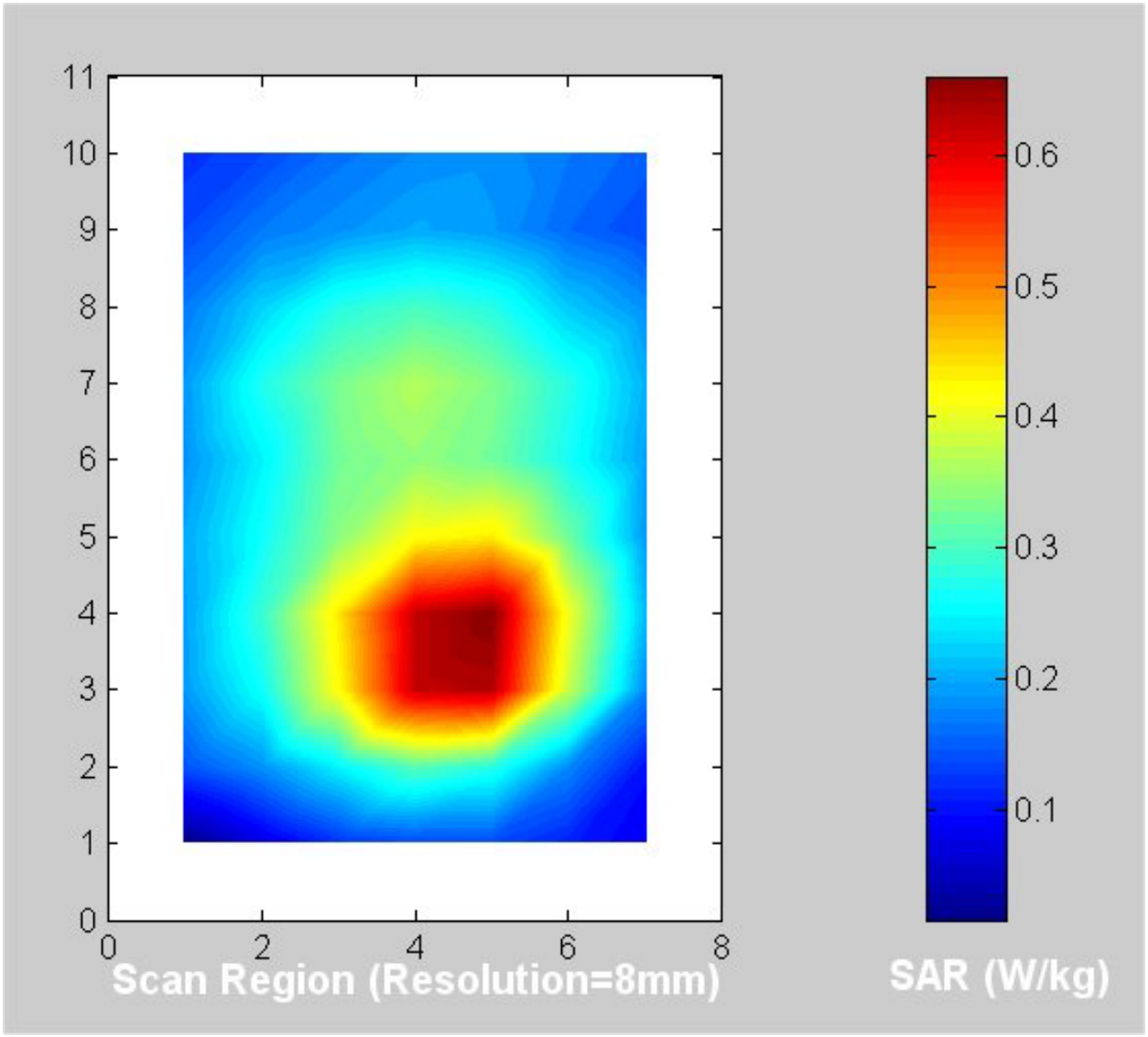

c. 5.29 GHz turbo mode – Main antenna (see Table 9 for the peak 1-g SAR).

Fig. 13. Coarse scans for the SAR measurements for the **Edge-On position** of the PC relative to the flat phantom **(Configuration 2,** see Fig. 4**)**. The right or the left edge of the PC with the 802.11a Main or Auxiliary antennas, respectively, was placed at 90° at a distance of 1.5 cm from the bottom of the flat phantom.

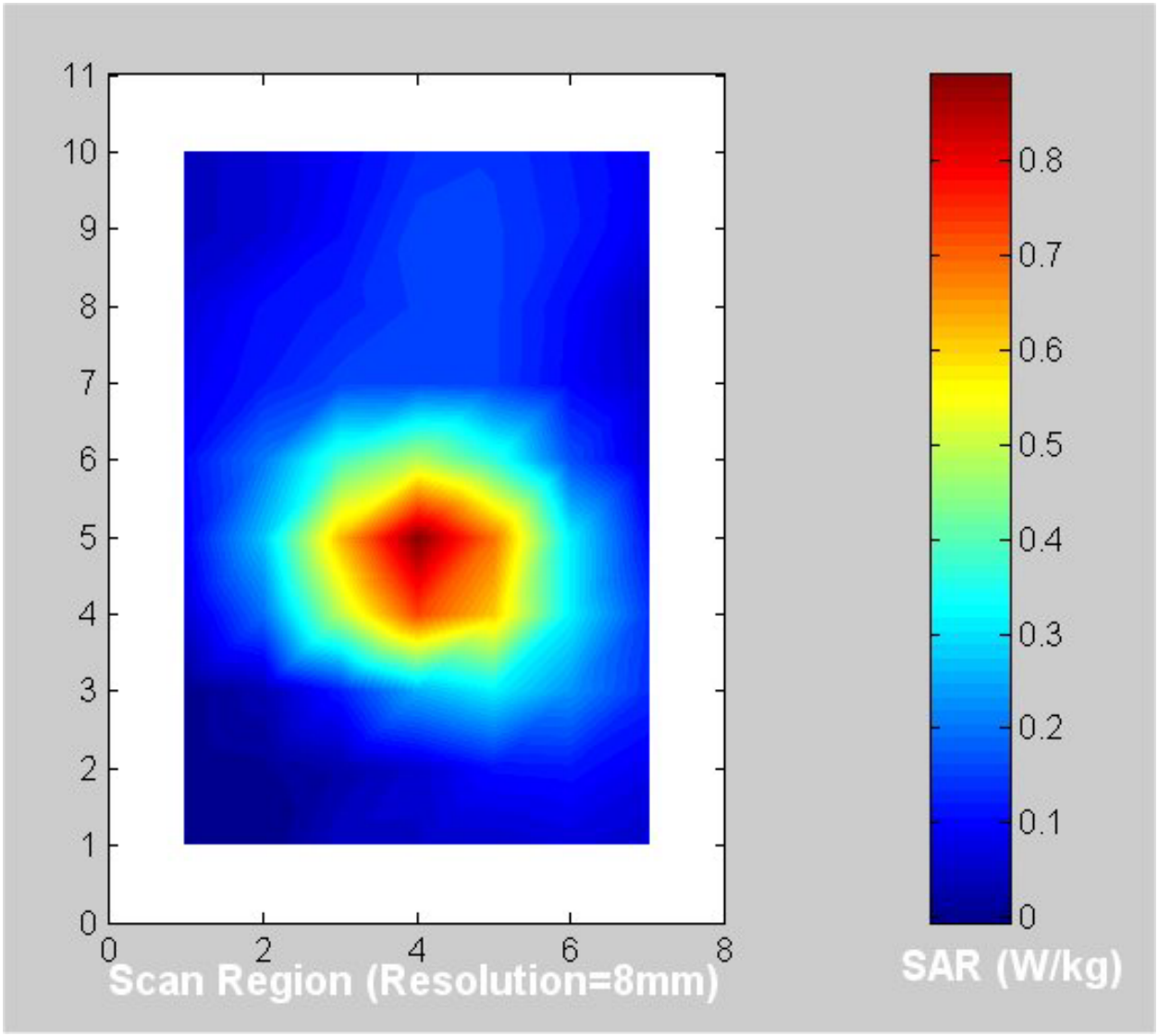

d. 5.29 GHz turbo mode – Auxiliary antenna (see Table 10 for the peak 1-g SAR).

Fig. 13. Coarse scans for the SAR measurements for the **Edge-On position** of the PC relative to the flat phantom **(Configuration 2,** see Fig. 4**)**. The right or the left edge of the PC with the 802.11a Main or Auxiliary antennas, respectively, was placed at 90° at a distance of 1.5 cm from the bottom of the flat phantom.

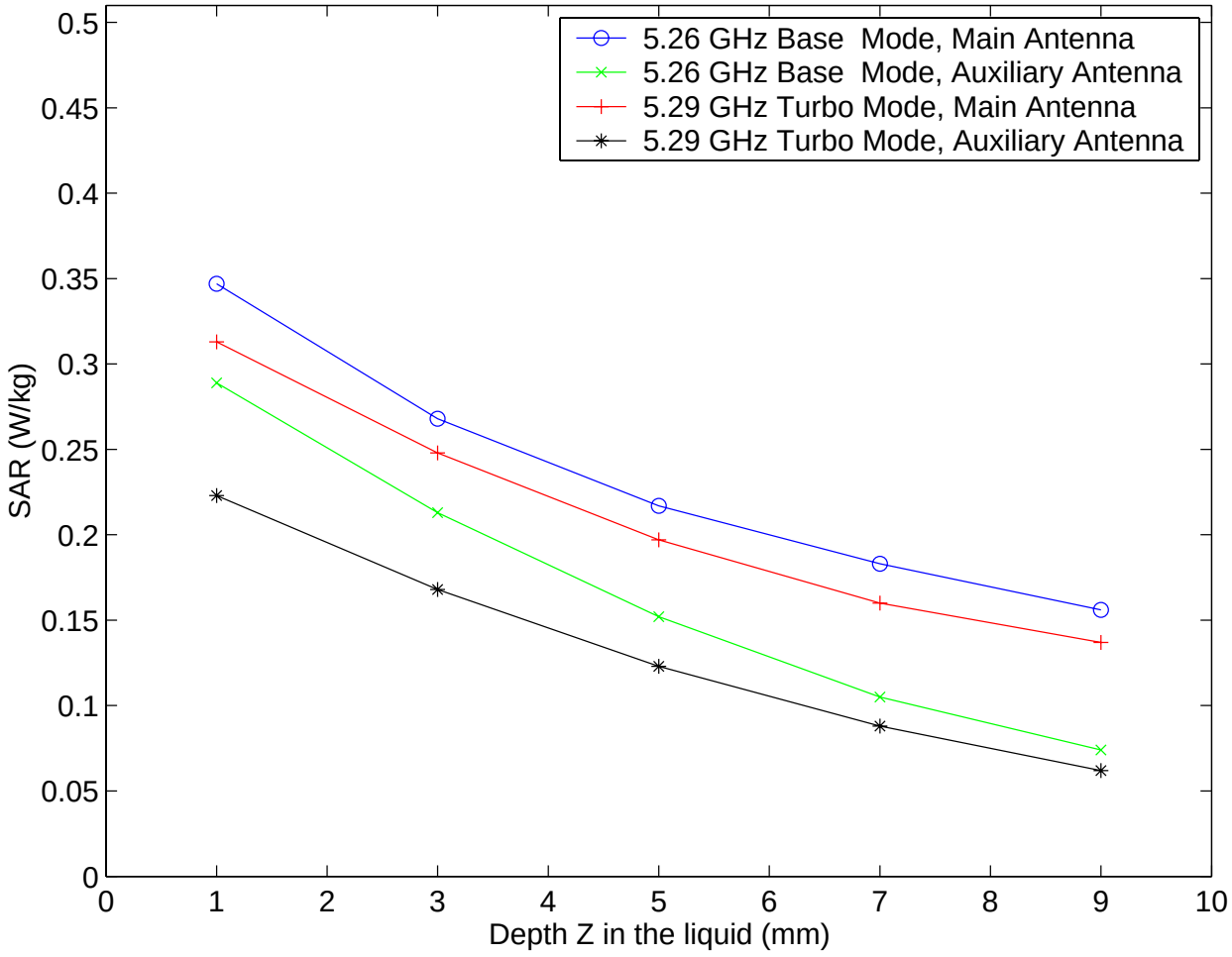

Fig. 14. Plot of the SAR variations as a function of depth Z in the liquid for locations of the highest SAR (from Tables 3-6 for **Above-Lap position**) for Wistron NeWeb EM-500 AG 802.11a Antennas built into Model BQ12 Notebook Computer.

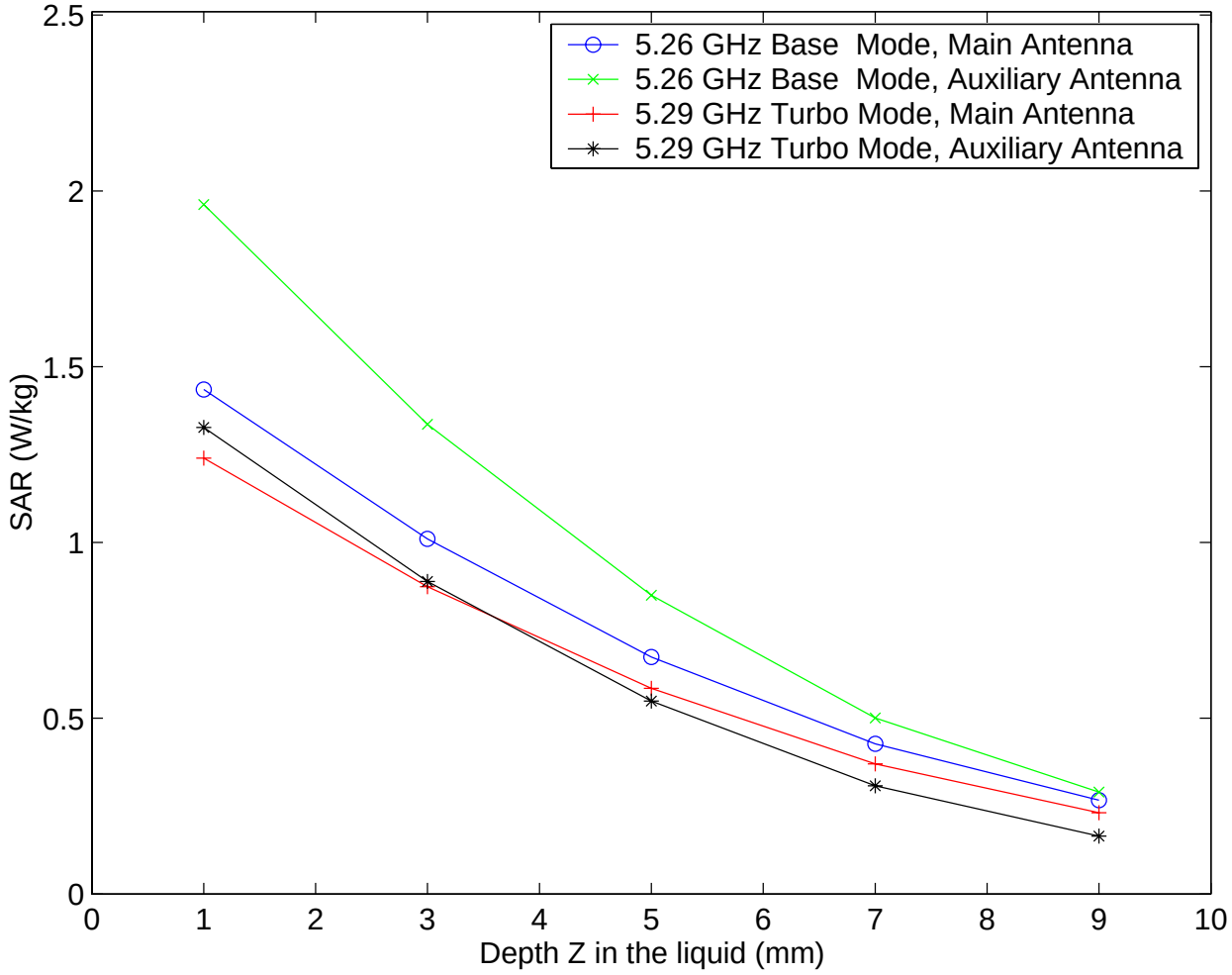

Fig. 15. Plot of the SAR variations as a function of depth Z in the liquid for locations of the highest SAR (from Tables 7-10 for **Edge-On position**) for Wistron NeWeb EM-500 AG 802.11a Antennas built into Model BQ12 Notebook Computer.

APPENDIX B

SAR System Verification for February 26, 2003

The measured SAR distribution for the peak 1-g SAR region using a dipole at 1900 MHz

For February 26, 2003 - The dipole SAR Plot

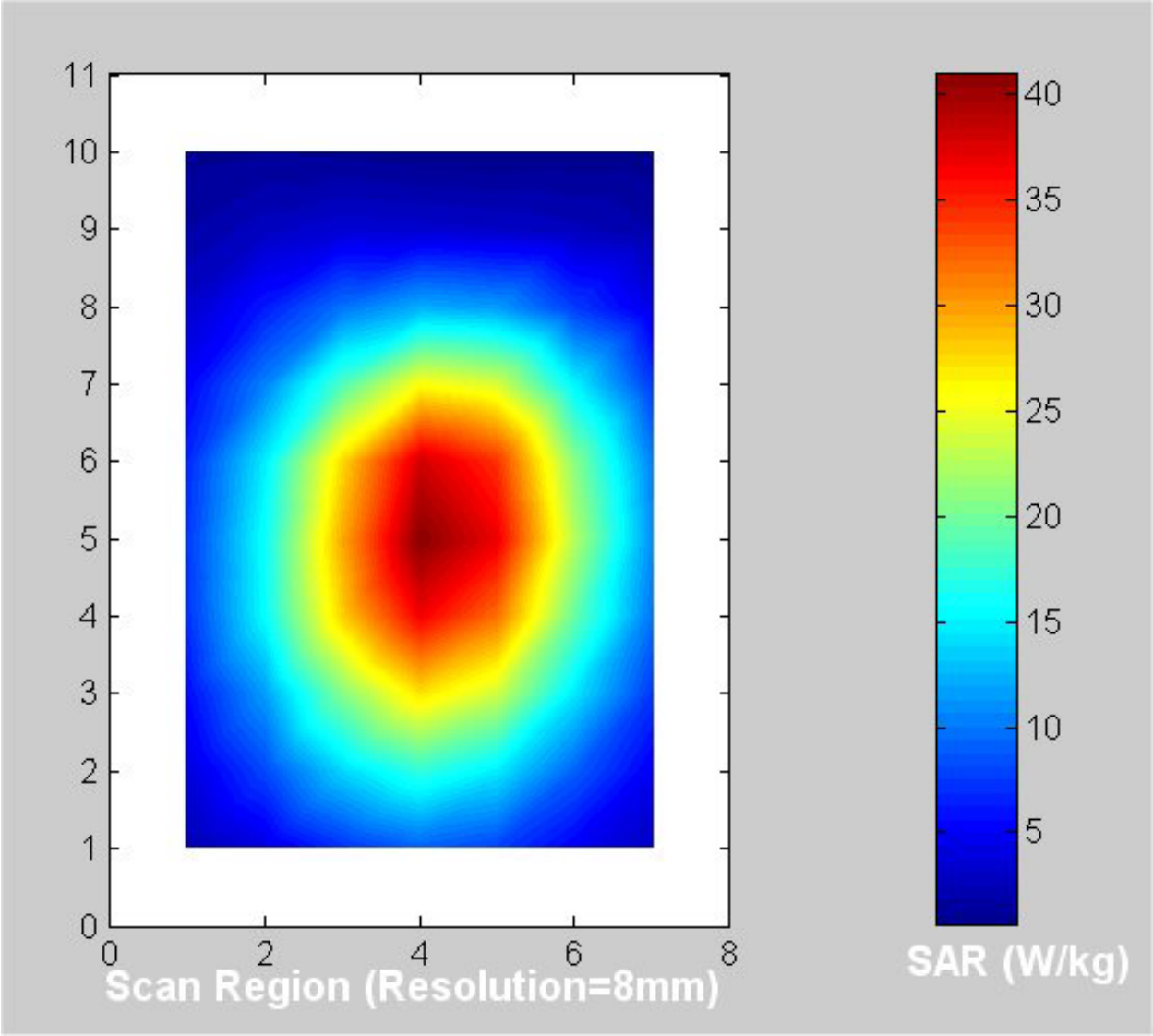

1-g SAR = 36.463 W/kg

a. At depth of 1 mm

55.298	57.456	58.093	56.810	54.034
56.406	58.591	59.312	58.583	55.649
56.358	58.756	59.787	58.886	56.289
55.788	58.172	59.234	58.641	56.129
54.811	57.245	58.506	57.910	55.353

b. At depth of 3 mm

43.327	44.877	45.331	44.456	42.415
44.254	45.839	46.393	45.817	43.706
44.360	46.087	46.798	46.160	44.246
44.016	45.738	46.529	46.067	44.199
43.326	45.092	45.961	45.509	43.649

c. At depth of 5 mm

33.222	34.283	34.594	34.040	32.607
33.990	35.086	35.498	35.056	33.616
34.201	35.382	35.839	35.413	34.059
34.029	35.214	35.779	35.428	34.092
33.571	34.790	35.352	35.023	33.731

d. At depth of 7 mm

24.983	25.674	25.882	25.560	24.609
25.616	26.332	26.627	26.301	25.378
25.881	26.639	26.911	26.645	25.729
25.825	26.600	26.986	26.724	25.809
25.547	26.339	26.677	26.453	25.599

e. At depth of 9 mm

18.610	19.049	19.194	19.017	18.422
19.130	19.579	19.782	19.552	18.993
19.401	19.861	20.013	19.855	19.256
19.405	19.897	20.148	19.955	19.350
19.252	19.738	19.937	19.799	19.253

APPENDIX C

Uncertainty Analysis

The uncertainty analysis of the University of Utah SAR Measurement System is given in Table A.1. Several of the numbers on tolerances are obtained by following procedures similar to those detailed in [8], while others have been obtained using methods suggested in [4].

Table B.1. Uncertainty analysis of the University of Utah SAR Measurement System.

Uncertainty Component	Tolerance ± %	Prob. Dist.	Div.	C_i 1-g	1-g u_i ± %
Measurement System					
Probe calibration	2.0	N	1	1	2.0
Axial istropy	4.0	R	$\sqrt{3}$	$(1\text{-}cp)^{1/2}$	1.6
Hemispherical isotropy	5.5	R	$\sqrt{3}$	$\sqrt{c_p}$	0.0
Boundary effect	0.8	R	$\sqrt{3}$	1	0.5
Linearity	3.0	R	$\sqrt{3}$	1	1.7
System detection limits	1.0	R	$\sqrt{3}$	1	0.6
Readout electronics	1.0	N	1	1	1.0
Response time	0.0	R	$\sqrt{3}$	1	0.0
Integration time	0.5	R	$\sqrt{3}$	1	0.3
RF ambient conditions	0	R	$\sqrt{3}$	1	0
Probe positioner mechanical tolerance	0.5	R	$\sqrt{3}$	1	0.3
Probe positioning with respect to phantom shell	2.0	R	$\sqrt{3}$	1	1.2
Extrapolation, interpolation, and integration algorithms for max. SAR evaluation	5.0	R	$\sqrt{3}$	1	2.9
Test Sample Related					
Test sample positioning	3	R	$\sqrt{3}$	1	1.7
Device holder uncertainty	3	R	$\sqrt{3}$	1	1.7
Output power variation - SAR drift measurement	5	R	$\sqrt{3}$	1	2.9
Phantom and Tissue Parameters					
Phantom uncertainty - shell thickness tolerance	10.0	R	$\sqrt{3}$	1	5.8
Liquid conductivity - deviation from target values	0.4	R	$\sqrt{3}$	0.7	0.2
Liquid conductivity - measurement uncertainty	1.5	R	$\sqrt{3}$	0.7	0.6
Liquid permitivity - deviation from target values	0.8	R	$\sqrt{3}$	0.6	0.3
Liquid permittivity - measurement uncertainty	3.5	R	$\sqrt{3}$	0.6	1.2
Combined Standard Uncertainty		RSS			8.3
Expanded Uncertainty (95% Confidence Level)					16.6